



Transforming the Carbon Economy: Challenges and Opportunities in the Convergence of Low-Cost Electricity and Reductive CO₂ Utilization

Journal:	<i>Energy & Environmental Science</i>
Manuscript ID	EE-PER-07-2019-002410.R1
Article Type:	Perspective
Date Submitted by the Author:	20-Oct-2019
Complete List of Authors:	Grim, Gary; National Renewable Energy Laboratory, National Bioenergy Center Huang, Zhe; National Renewable Energy Laboratory, National Bioenergy Center Guarnieri, Michael; National Renewable Energy Laboratory, National Bioenergy Center Ferrell, Jack; National Renewable Energy Laboratory, National Bioenergy Center Tao, Ling; NREL, ; National Renewable Energy Laboratory, Schaidle, Joshua; National Renewable Energy Laboratory, National Bioenergy Center



PERSPECTIVE

Transforming the Carbon Economy: Challenges and Opportunities in the Convergence of Low-Cost Electricity and Reductive CO₂ Utilization

Received 00th January 20xx,
Accepted 00th January 20xx

DOI: 10.1039/x0xx00000x

R. Gary Grim,^a Zhe Huang,^a Michael Guarnieri,^a Jack Ferrell,^a Ling Tao^{a*} and Josh Schaidle^{a*}

The increasing availability of renewable electricity at costs competitive with, and even lower than, electricity from fossil sources along with growing interest and recent technological advancements in reducing carbon emissions through CO₂ capture is challenging the status quo in the way that we produce and consume energy and products. Renewable electricity can be leveraged to produce fuels and chemicals from CO₂, offering sustainable routes to reduce the carbon intensity of our energy and products-driven economy. A number of approaches have been developed for the electron-driven reduction of CO₂ to products, including both direct and indirect (via an energy carrier such as H₂) pathways and spanning from electrochemical to biological to thermocatalytic conversion. While these approaches are at various stages of development, there are technical barriers related to each core conversion technology that need to be addressed in order to accelerate commercialization and drive the transition towards a circular carbon economy. In this perspective, we assess and characterize the top technical barriers for utilizing renewable electricity for CO₂ reduction across five different conversion approaches (direct electrochemical, direct bioelectrochemical, direct non-thermal plasma, indirect bioelectrochemical, and indirect thermochemical) under state-of-technology conditions, outline the R&D needs to overcome each barrier, and identify the most promising C₁-C₃ hydrocarbons and oxygenates based on their relative ease of formation, economic viability, CO₂ utilization potential, and energy storage capacity. Our analysis suggests, based on current reported states of technology, that indirect pathways paired with the formation of C₁ products offer the most technically feasible approach for electron driven CO₂ reduction in the near term. However, as we strive for longer carbon chain molecules, and as technologies continue to advance, there are a multitude of pros and cons to be considered for all five approaches.

Introduction

In 2017, global CO₂ emissions eclipsed 36 gigatonnes (GT), equating to a loss of nearly 10 GT of carbon to the environment.¹ This continued release of CO₂ highlights the unsustainability of the current linear carbon economy. Although technologically viable methods for CO₂ capture and sequestration are available, the low intrinsic value of CO₂ and relatively high capture costs have limited market adoption in the absence of policy or economic incentives (e.g., federal credits and enhanced oil recovery). As an example, post-combustion carbon capture and storage (CCS) is a commercially available technology, yet of the tens of thousands of global point sources suitable for CCS, only 23 large-scale facilities were either in operation or under construction worldwide as of 2018, contributing to a reduction of only ~40 million metric tonnes of CO₂ per year (MMT/y) or approximately 0.1% of total global emissions.²

An alternative to storage is the purposeful utilization of CO₂ as a feedstock for the synthesis of fuels and chemicals. Reuse of CO₂ provides a revenue stream that offsets capture costs and may even generate positive cash flow.³ However, due to the high degree of

oxidation and thermodynamic stability of CO₂, reductive conversion processes are energy intensive.⁴⁻⁶ To provide context, based solely on reaction thermodynamics, the electrochemical conversion of CO₂ to CO at standard conditions requires approximately 18.4 GJ/tonne CO assuming a 50% energy efficient conversion process (Table S1), ranking it amongst other known energy-intensive commercial processes such as steel production (21 GJ/tonne),⁷ ammonia synthesis (28.1-35.5 GJ/tonne)*,⁸ and petrochemical ethylene production (26 GJ/tonne)*.⁹ To realize a circular carbon economy, this energy demand for CO₂ reduction (CO₂R) would need to be met by low-carbon and low-cost electricity.⁶

Presently, the increasing availability of high-purity CO₂ containing waste streams (e.g., bioethanol refineries) combined with electricity from renewable sources reaching cost parity with coal or natural gas-derived power (Fig. 1a) is challenging the status quo in the way that we produce, convert, and consume energy and products. In locations with abundant wind and solar resources, discounted and in some cases

^a National Renewable Energy Laboratory, 15013 Denver W Pkwy, Golden, CO 80401

*Corresponding Author: ling.tao@nrel.gov, josh.schaidle@nrel.gov
Electronic Supplementary Information (ESI) available: [details of any supplementary information available should be included here]. See DOI: 10.1039/x0xx00000x

*LHV assumed in the calculation if not specified; GJ/tonne is the energy consumption per tonne product.

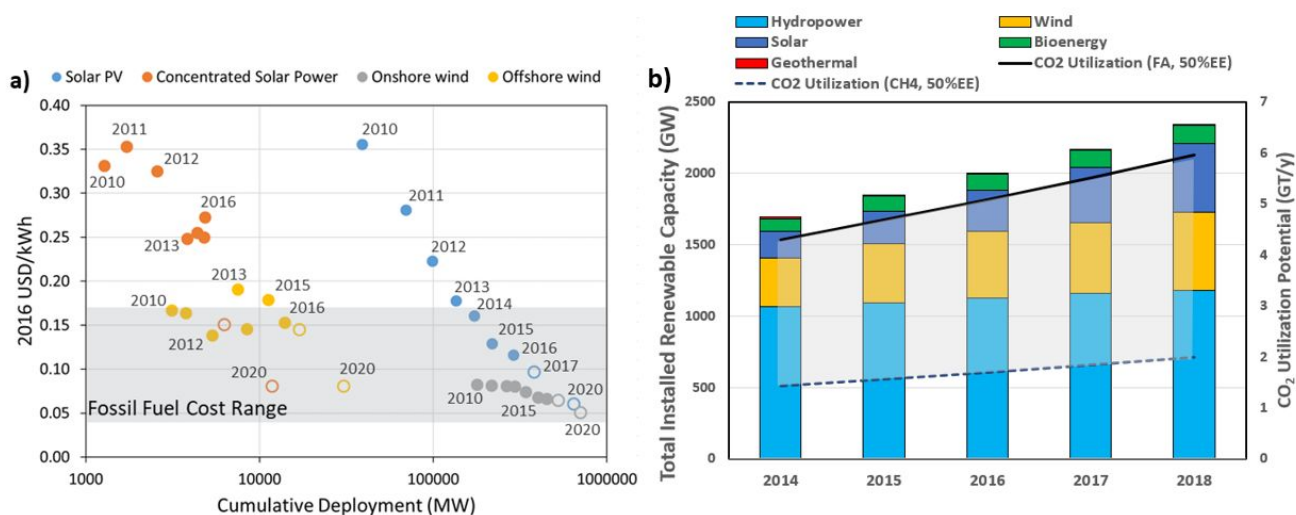


Figure 1a: Levelized cost of solar and wind derived power versus deployed capacity. Closed and open circles represent reported and projected data respectively. Source: IRENA.¹⁰ 1b: Installed renewable electricity capacity from 2014-2018 with estimated potential for CO₂ utilization in GT/y assuming electricity and CO₂ converted to formic acid (solid line) or CH₄ (dashed line) at 50% energy efficiency. Modified from¹¹.

negative energy prices present compelling economic opportunities for sustainable CO₂R to products.¹² Although still the minority, renewable energy sources now comprise approximately 25% of the global electricity capacity, providing a huge opportunity for CO₂R.¹³ Specifically, at the end of 2018, the International Renewable Energy Agency (IRENA) estimated 2,351 GW of installed global renewable energy generation across wind, solar, hydroelectric, and other sources.¹¹ If this capacity were directed toward electrochemical CO₂R for example, approximately 2-6 GT/y of CO₂ (see supplementary information) could be converted to products, depending on the energy efficiency of the conversion pathway and targeted product (Fig 1b). To put this potential for CO₂ utilization in perspective, the global production of ethylene is *ca.* 77 MMT/y, which on a CO₂ basis (i.e., 2 mol CO₂ to 1 mol C₂H₄) comprises only 121 MMT/y CO₂.

Compared to conventional fossil-based processes, CO₂R pathways, driven by renewable electricity, offer a number of potential benefits, including (1) reducing the carbon intensity of the end products, (2) acting to stabilize the electric grid through consumption of variable and otherwise curtailed electricity, and (3) offsetting CO₂ capture costs, all while accessing most fuel and chemical products traditionally synthesized from petroleum. Shown in Fig. 2, CO₂R pathways can utilize electricity directly in the conversion step or indirectly via other energy carriers (e.g., H₂). Currently accessible conversion pathways include electrochemical, bioelectrochemical, non-thermal plasma (NTP), and thermochemical conversion. In electrochemical pathways, CO₂R is controlled by applied potential, electrolyte, cell design, and inorganic electrocatalyst properties (e.g., metal type, surface characteristics). Bioelectrochemical pathways forego metal catalysts on the cathode and fix CO₂ via metabolic pathways within microorganisms, using electrons directly or indirectly through other reducing agents (e.g., H₂). NTP pathways utilize electrical energy to selectively excite electrons at near ambient temperature and pressure conditions to initiate reductive chemistry. Thermochemical routes leverage high temperatures and pressures over metal- and metal oxide-based catalysts to hydrogenate CO₂ through established chemical pathways. CO₂ can also be utilized non-

reductively through commercially mature routes such as enhanced oil recovery, food and beverage, and concrete curing (Fig. 2). While these non-reductive routes have a higher relative level of maturity, there are fewer opportunities for electricity utilization compared to reductive routes. As this perspective emphasizes technological challenges and opportunities in the utilization of renewable electricity and CO₂, emerging lower technology readiness level (TRL) reductive processes are the focus of this work.

The convergence of low-cost renewable electricity and the growing global push for reducing the carbon intensity of our economy^{3, 14-16} has created the ideal environment for CO₂R to flourish; however, a myriad of technical challenges exist for these technologies that need to be overcome to accelerate market adoption. In this perspective, we assess the technical feasibility and establish the state-of-technology (SOT) of all current CO₂R pathways (direct electrochemical, direct bioelectrochemical, NTP, indirect bioelectrochemical, indirect thermochemical) highlighted in Fig. 2.

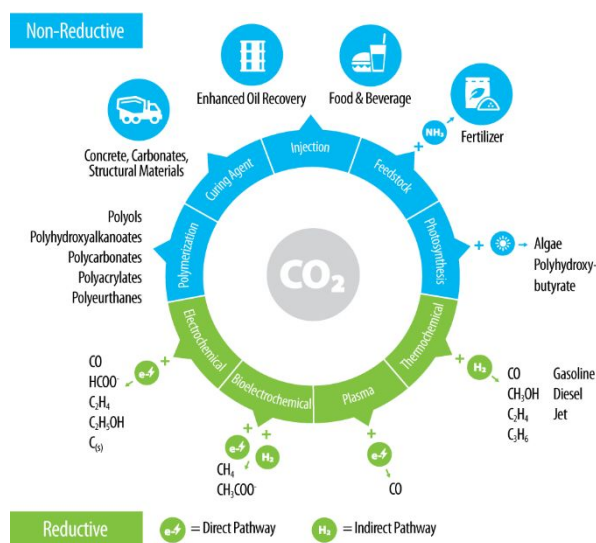


Figure 2: Reductive and non-reductive pathways for CO₂ utilization shown with major products. Only reductive pathways are considered in this study.

In evaluating the respective figures of merit for each pathway, we compare the relative TRL (see Table S6 for definitions), highlight the top technical barriers, and discuss the most critical R&D advancements needed to accelerate the deployment of these technologies. While policy and economic drivers will also influence CO₂R adoption, they will not be discussed. We also evaluate 22 C₁-C₃ species¹⁷ accessible via CO₂R in terms of the relative ease of formation, market potential, CO₂ utilization potential, and energy storage capacity, to identify the most promising near-term targets. While individually CO₂R pathways have been studied and reviewed,¹⁸⁻²¹ we compare the advantages and disadvantages of multiple pathway-product combinations and highlight opportunities for transformational R&D by evaluating the rapidly evolving SOT of each pathway. These key findings serve as a first-of-a-kind guide for the near- and long-term development of these diverse CO₂R technologies.

Direct Electrochemical

Overview

In the direct electrochemical reduction of CO₂, an external voltage is applied across a pair of electrodes whereby CO₂ can be reduced to products encompassing solid carbon, hydrocarbon, and oxygenated species. Depending on operating temperature and ion transport medium, multiple electrolyzer configurations can be utilized (Fig. 3).²² Below 100 °C, aqueous electrolyte electrolyzers and membrane electrode assemblies (MEA) are the most common designs. Aqueous electrolyzers rely on dissolved CO₂ within an aqueous electrolyte whereby cations or anions are selectively passed through a membrane dividing cathode and anode. MEAs favor a more compact "stack" design utilizing cation or anion conducting polymer-based electrolytes and typically involve tailored flow-fields and gas diffusion electrodes (GDE) to increase the diffusivity of CO₂ thereby raising the concentration at the electrocatalyst surface. At higher temperatures (>400 °C) ceramic-based membranes conduct protons

or O²⁻ species depending on reactor configuration and utilize sensible heat to lower overall reduction potentials. More than 20 reduced products have been reported during electrochemical CO₂R comprising alcohols, aldehydes, ketones, carboxylic acids, glycols, alkenes, and alkanes.^{23, 24} With over three decades of research and development,²⁵ select CO₂ electrochemical technologies are nearing breakthrough on the commercial level highlighted by recent high-temperature electrolytic production of CO up to ~200 Nm³/hr for specialty gas applications using a O²⁻ conducting solid oxide electrochemical cell (SOEC).²⁶ However, the formation of higher value products requiring the coupling of carbon-carbon bonds still faces many technical challenges.

Direct electrochemical processes (and direct bioelectrochemical discussed below) are commonly evaluated based on at least three metrics: current density, overpotential, and faradaic efficiency as defined below. To benchmark the SOT of each direct pathway, a comparison to proton exchange membrane (PEM) and alkaline water electrolyzers are also provided. Water electrolyzers represent a comparatively well-studied and commercially scaled up pathway for the conversion of electricity to chemical bonds, offering the most like-for-like comparison. In Table 1 the SOT metrics of H₂ derived from water electrolysis and 18 CO₂R electrochemical products are shown. Studies were selected as "SOT" based on the highest reported cathodic partial current density. Partial current density provides a measure of the number of electrons consumed for a specific product per area of electrode per time and provides an estimate of productivity based on current technology. Energy efficiencies (ϵ) are calculated from Equation 1, where ΔG is the change in Gibbs free energy, T is operating temperature, ΔS is the change in entropy, FE_i is the faradaic efficiency of species *i*, η is the overpotential (V), *n* is the number of mols of electrons transferred (e.g., 2 for CO), and F is Faraday's constant.²⁷

$$\epsilon_{energetic} = \frac{(\Delta G + T\Delta S) \cdot FE_i(\%)}{\Delta G + \eta n F} \quad (1)$$

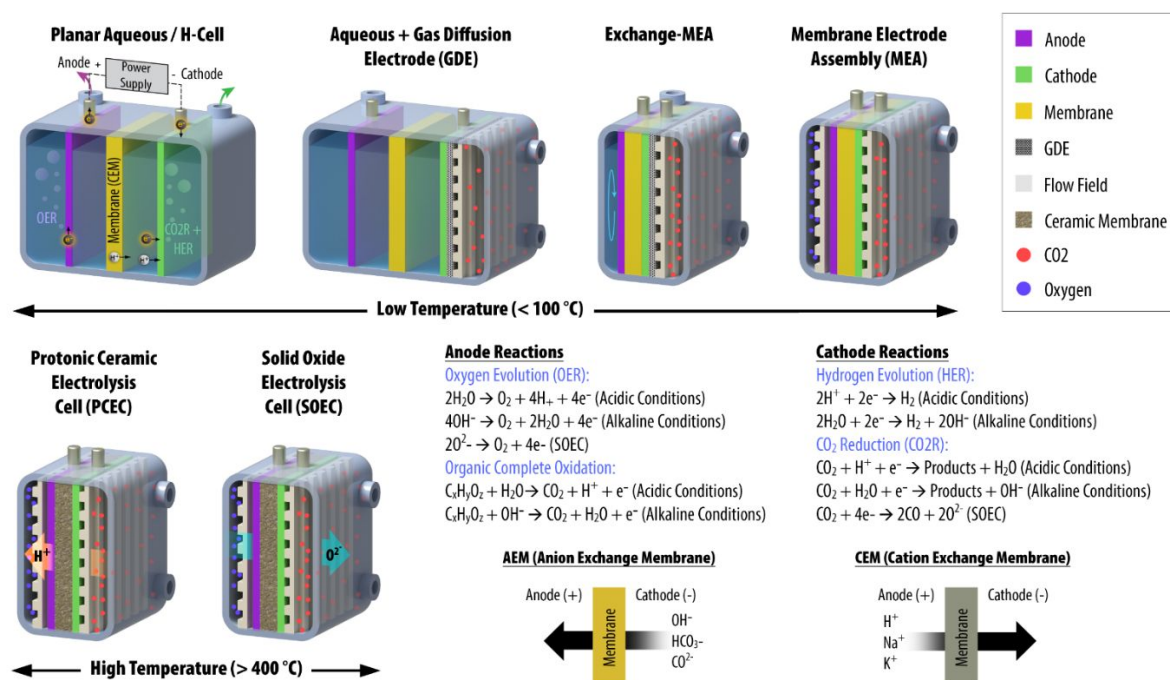


Figure 3: Overview of CO₂R electrolyzer configurations with general oxidation and reduction reactions.

Table 1: Summary of SOT metrics for electrochemical reduction of CO₂ to 18 products. CO₂R products are sorted in descending value of partial current density.

Species	#e	Std. Potential vs. SHE @ pH7 (V)	η (mV)	j_{partial} (mA/cm ²)	FE (%)	ϵ^a (%)	Ref
Hydrogen (PEM)	2	-0.41	570 ^d	2,000	100 ^b	68-71	28, 29
Hydrogen (Alkaline)	2	-0.41	570 ^d	400	100 ^b	62-82	28
Carbon Monoxide (HT, SOEC) ^c	2	-0.51	670 ^d	870	99.9	88.6	30
Ethylene	12	-0.32	750 ^e	473	63.0	35.2	31
Carbon Nanotubes	4	-0.20	2180 ^{d,f}	327	81.7	28.2	32
Carbon Monoxide (LT, Aq.)	2	-0.51	1670 ^d	350	~100	45	33
Formic Acid	2	-0.59	1140 ^e	177	88.3	42.3	34
Ethanol	12	-0.33	768 ^e	80	26.0	13.9	35
Oxalic Acid	2	-0.94	4980 ^{d,g}	37.5	50.0	11.4	36
1-Propanol	18	-0.31	1360 ^e	30.6	5.1	2.1	37
Acetic Acid	8	-0.32	890 ^e	18	3.0	1.9	37
Methane (LT, Aq.)	8	-0.24	1520 ^e	9.3	76.0	30.6	38
Methanol	6	-0.39	150 ^e	~0.2	98.0	74.0 ^h	39
Allyl Alcohol	16	-0.36	1120 ^e	0.06	1.6	0.7	23
Glycolaldehyde	8	-0.47	1110 ^e	0.07	0.62	0.3	23
Acetaldehyde	10	-0.35	1100 ^e	0.02	0.34	0.2	23
Propionaldehyde	16	-0.33	1150 ^e	0.017	0.48	0.2	23
Ethylene Glycol	10	-0.40	1290 ^e	0.013	0.15	0.1	23
Acetone	16	-0.31	950 ^e	0.007	0.08	< 0.1	23
Hydroxyacetone	14	-0.36	1470 ^e	0.001	0.04	< 0.1	23
Glyoxal	6	-0.62	n.d.	n.d.	n.d.	n.d.	23

a: Electrolyzer stack energy efficiency calculated based on Equation 1. Calculations shown in Table S4. Unless stated, whole cell reaction potential assumes H₂O splitting on anode at 1.23V with +300 mV overpotential based on SOT data.⁴⁰ Actual ϵ may be lower if process boundaries expanded to include additional unit operations.

b: Neglects resistive losses

c: SOEC experiment performed at 800 °C

d: Whole cell overpotential

e: Cathodic overpotential

f: Whole cell voltage of ~3.2 V

g: Whole cell voltage ranged from 5.7-6.5 V

h: Low current density promotes high ϵ at tradeoff of productivity. Not expected to be characteristic of realistic ϵ .

Current Density (j): The electron flux per unit area (mA/cm²) of an electrode is denoted as current density. Maximizing current density is essential to reducing the size and capital cost of reactors, especially in systems with poor selectivity. SOT PEM water electrolyzer systems demonstrate current densities >2000 mA/cm².²⁸

Overpotential (η): In practice the experimentally observed potential is greater than the thermodynamically determined value (E^{n}) due to internal resistances related to mass transfer (η^{mt}), ohmic resistances (η^{ohm}), and activation barriers (η^{act}).³⁹ The difference between observed and thermodynamic potentials is denoted as overpotential (η) and represents energy loss within the system. A large overpotential raises operating costs, reduces efficiencies, and if high enough can damage both electrocatalysts and catalyst supports.⁴¹⁻⁴³

In modern PEM water electrolyzers, cathodic and anodic overpotentials are approximately +300 mV across SOT studies, depending on current density.^{40, 44}

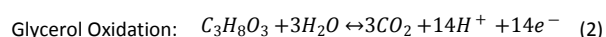
Faradaic Efficiency (FE): Faradaic efficiency represents the ratio of electrons utilized in a desired product to the total electrons input into the system. Because of high overpotentials observed experimentally in electrochemical reduction reactions, multiple products are often thermodynamically favorable (Table 1), leading to side reactions such as hydrogen evolution (HER) and in the case of Cu electrodes, multiple carbon products (Fig. 4). In modern PEM water electrolyzer systems, ~100% faradaic efficiency has been demonstrated.⁴⁵

Technical Challenges

Improving Energy Efficiency and Reducing Cell Overpotential:

Aside from CO derived from high-temperature electrolysis at 89%, demonstrated energy efficiencies across electrochemical products typically falls between 0.1–45%. By comparison, commercial routes for CO₂ and/or electron utilization such as thermochemical catalytic hydrogenation of CO₂ to methanol and water electrolysis have reported net energy efficiencies in the range of 50-70%.⁴⁶⁻⁴⁸ Lower energy efficiency contributes to higher production costs. Contributing factors to the low observed energy efficiencies, especially in the case of C₂₊ products, are low faradaic efficiencies and the high overpotential required to reach relevant current densities (i.e., on the order of 100s mA/cm²).^{4, 22, 49} As an example, in recent studies with polycrystalline Cu catalysts, to synthesize C₂₊ species with current densities > 1 mA/cm² in an aqueous electrolyte alkaline cell, cathodic overpotential in excess 500-800 mV was required.^{50, 51}

Additionally, at 1.23 V vs. SHE the thermodynamic potential of the anodic H₂O oxidation reaction is 1130 – 1330 mV higher than the cathodic half-cell potential required to form most reduced species. The oxidation product (O₂) also has limited situational value (e.g., co-location with oxy-combustion power generation) which under most circumstances is not easily marketable at scale for co-product credit. Thus, despite advantages in sourcing, conventional H₂O oxidation at the anode also contributes to a significant increase in absolute cell potential ($E^{\circ}_{\text{cell}} = E^{\circ}_{\text{cathode}} - E^{\circ}_{\text{anode}}$). Alternatively, potential substitutes for H₂O oxidation have been suggested such as low-cost organic substrates, chloride ions, or wastewater.^{52, 53} Although potentially more restrictive in terms of availability, and pricing, the thermodynamic potential required to oxidize organic species such as ethanol, ethylene glycol, or glycerol is significantly lower than the oxygen evolution reaction (OER) at 0.08, 0.03, and 0.003 V respectively vs. SHE.⁵⁴ Further, if complete oxidation at the anode is achieved (Eq. 2), CO₂ is produced which could theoretically be recycled to the cathode, thereby reducing feedstock costs. For partial oxidation, semi-reduced species (e.g., acetaldehyde and acetic acid) can be recovered for downstream processing or sale, enhancing the overall process economics.⁵⁵ However, the realistic scale at which organics could be sourced and the economic feasibility of CO₂ capture and recycle from oxidation should be carefully evaluated.



To reduce overpotential and increase the energy efficiency of electrocatalysts, the effect of ionic electrolytes,⁵⁶ soluble co-catalysts (e.g., pyridine),⁵⁷ electrocatalyst surface properties,⁵⁸ and optimization of reaction conditions (e.g., reactor design, solvent, pH, mass transport effects) has been studied.^{31, 35} Specific areas of interest with respect to electrocatalyst development include effect of particle size,⁵⁹ surface roughness,⁵⁸ expression of targeted crystal facets,⁶⁰ formation of nanostructures,⁵¹ electrolyte pH,³¹ and metal/alloy type.^{50, 61} Future R&D should continue exploring optimization of electrocatalysts, consider substitutes for H₂O oxidation, and where possible, leverage the advancements of earlier overlapping efforts in H₂O electrolysis / fuel cell R&D.

electrocatalyst, but also the role of electrolyte, flow fields, pH, and mass transport. Future R&D should continue emphasizing these

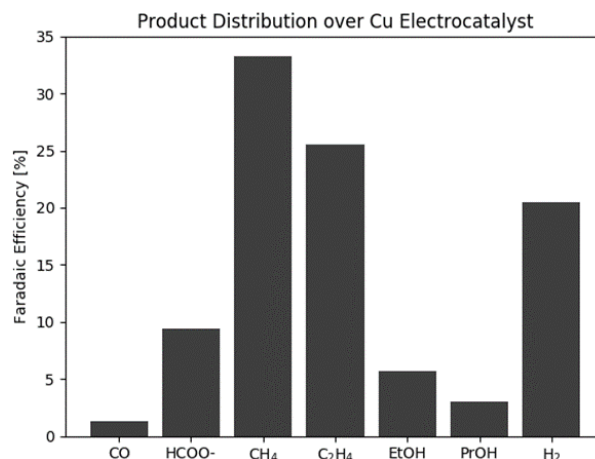


Figure 4: Reported product distribution of a single experiment over polycrystalline Cu.⁶²

Forming Carbon-Carbon Bonds with High Faradaic Efficiency:

With the reduction potential of most CO₂-derived products within ± 200 mV of the hydrogen evolution reaction (HER) as shown in Table 1, competing pathways to products and parasitic side reactions represents a major challenge to electrochemical selectivity. With previous work identifying the optimal cell voltage range for creating C-C bonds over Cu electrocatalysts as approximately -1.11 to -1.41 V versus SHE (pH 7), all C₂₊ products are thermodynamically favorable under normal reaction conditions.⁶³ This challenge is clearly demonstrated from work by Hori et al. showing the formation of 7 products in a single experiment over Cu at 5 mA/cm² and -1.44 V vs. SHE (Fig. 4).

Improved faradaic efficiencies to C₂₊ products has been recently reported using a new class of “oxide-derived” Cu catalysts comprised of continuous metal films containing 10-100 nm crystallites producing C₂-C₃ species at up to 57-70% cumulative faradaic efficiency at cell voltages ranging from -0.71 to -1.41 V versus SHE (pH 7).⁶³⁻⁶⁵ Hori et al. investigated Li⁺, Na⁺, K⁺ and Cs⁺ cationic species with HCO₃⁻ showing that as cation size increased, products had at higher C₂/C₁ ratio, lower selectivity to HER, and lower required potential^{63, 66}. Additional areas of interest include promoting specific surface facet sites (Cu[100] vs. Cu[111]),⁶⁷ increasing number of grain boundaries,⁶⁵ reducing crystallite size,⁶⁸ and controlling local pH.⁶³

Across SOT studies the cumulative faradaic efficiency to C₂₊ products has now reached levels in excess of 80% at 275 mA/cm² compared to 34% reported in initial discovery by Hori et al.^{31, 62} These advancements, as noted, have been achieved by breakthroughs in surface science, materials synthesis, and a push towards flow cell reactor configurations. However, reaching comparable faradaic efficiencies for individual C₂₊ products to that observed with C₁ chemistry (i.e., > 90% FE at > 100 mA/cm², Table 1) has yet to be demonstrated. Thus, while electrocatalyst advancements have contributed to improvements in C₂₊ selectivity, the best performing catalysts to date are still based on Cu similar to the initial discovery by Hori et al. nearly three decades ago. The most impactful studies moving forward will consider not only development of the

complementary fields along with the effect of surface morphology to better direct product selectivity.

Controlling pH and Carbonate Formation:

Depending on catalyst morphology, mass transfer rates, and buffering capacity of the electrolyte, the pH at the interface of the electrolyte and electrocatalyst can rise above that of the bulk due to rapid hydroxide anion release during CO₂ reduction.^{49, 63} This gradient in interfacial pH and increase in electrolyte alkalinity is positively correlated with higher C₂₊ product selectivity over Cu electrodes due to the low concentration of protons and slow kinetics in the Volmer adsorption step thereby suppressing the competing HER reaction.^{31, 63, 69, 70} However, hydroxide anions released during the reduction reaction (or present in the bulk electrolyte) scavenge CO₂ molecules in solution forming HCO₃⁻ or CO₃²⁻, lowering the concentration of available CO₂, limiting reaction rates, and reducing effective carbon conversion.^{63, 71}

The impact of interfacial ion gradients and depletion of dissolved CO₂ can be minimized at low current density typically found in lab-scale studies (i.e., < 10 mA/cm²); however, as commercially relevant current densities are probed, maintaining stable ion concentrations (pH) in the boundary layers near the electrode surface will be even more challenging. If alkaline operation is preferred, as typical with most SOT studies,^{31, 35, 37} HCO₃⁻ and CO₃²⁻ accumulation within the cathode and/or transport across the AEM and subsequent oxidation to CO₂ on the anode must be considered from the perspective of lower carbon conversion. Recent efforts by Dinh et al. minimize CO₂ losses using GDE-based alkaline electrolyzers with “abrupt interface geometries” and short diffusion lengths; however, at the expense of single-pass CO₂ conversion.³¹ Further research is needed in this area to suppress HER formation under more acidic conditions thereby minimizing carbonate formation, and/or in process development for the purification and recycle of carbonate species in effort to improve net carbon efficiencies and minimize CO₂ losses.

Reactor Design Standardization, Stability Testing, and Data Reporting

Due to ease of operation and ambient reaction conditions, the most common reactor used in academic studies is the aqueous three-electrode “H-cell” (Fig. 3). However, in relying upon aqueous electrolytes and atmospheric pressure, H-cell systems suffer from low CO₂ solubility and limited scalability. Applying a semi-infinite diffusion model, Martin et al. show that aqueous systems in equilibrium with pure CO₂ at 1 bar and 25 °C would have a maximum attainable current density of only 60 mA/cm² under vigorous stirring conditions.³⁹ Further, the relatively large distances separating anode and cathode compartments contribute to large ohmic losses (i.e., higher overpotential), making it an impractical choice for commercial high current density operation.²²

One option for overcoming these limitations are “flow-cell” membrane-electrode-assemblies (MEA) paired with gas diffusion electrodes that increase CO₂ diffusivity and concentration at the electrode interface, thereby raising current density and productivity. However, MEA reports comprise only a small minority of the electrochemical literature with Weekes et al. showing that between 2007-2017 there were 51 studies conducted using H-cells for each flow-cell study (21 total).⁷² Recognizing that future at-scale designs will likely operate under harsher conditions, higher pressure, higher

current density, have different flow fields, and various electrolytes compared to the H-cell system, there is a lack of understanding around how well, or if at all, the electrocatalytic performance will translate to the more commercially relevant reactor designs.⁴⁹ Consequently, there is a need to accelerate the shift towards more commercially relevant reactor designs and scales^{48, 53} while also developing standardized testing protocols by which a like-for-like comparison can be made across difference designs to determine how process metrics will translate.

Electrocatalyst deactivation is impacted by a multitude of operational parameters that can manifest in agglomeration of nanomaterials thereby reducing active surface area, poisoning of surface sites, and corrosion of support materials.⁴¹⁻⁴³ However, with most academic studies focused basic science, data on process stability is scarcely reported for CO₂ reduction, if at all. Accordingly, most reported SOT process stabilities are on the order of only one to tens of hours,⁴ well short of the targeted tens of thousands of hours demonstrated commercial electrolyzers.²⁹ This gap in knowledge represents a significant barrier to commercialization requiring immediate action with respect to development of accelerated testing procedures to quickly identify failure mechanisms and inform the rational design of materials that are both active and durable over prolonged periods.

Finally, quantifying year over year incremental improvements related to electrochemical R&D is often challenging in that the conditions under which data are recorded are often inconsistent with respect to catalyst type, electrode preparation methods, reactor configuration, and operating conditions.⁴ Direct comparisons are further complicated by the way in which results are often conveyed. Publications too often neglect to report important applied data (e.g. single pass conversion) or selectively highlight incremental improvements in overpotential, faradaic efficiency, or current density when in reality, the metrics are independently observed under different reaction conditions. Although improvements may be made to an individual metric, if observed at the expense of sacrificing other equally important commercial metrics, it is difficult to meaningfully assess the net contribution to advancing the underlying technology. Across academia and industry, there is an immediate need to establish a standardized set of guidelines for electrochemical testing and reporting of data. Under consistent operational conditions it will be possible to determine the effect of variables on a like-for-like basis, accelerating the quality and rate of advancements in this space.

Non-Thermal Plasma

Overview

Known as the 4th state of matter, plasma is defined as a state of ionized gas.⁷³ In non-thermal plasmas (NTP), the comprising species exist in a state of non-local thermodynamic equilibrium (non-LTE) in which the electron temperature is significantly higher compared to that of the heavier neutral or ionized gas molecules.^{21, 74} In NTP, electrons are typically energized to 1 – 10 eV which is considered the optimum range for breaking chemical bonds (5.5 eV for OC=O), otherwise requiring high temperatures/pressures under traditional thermocatalytic approaches.⁷⁵ NTP processes also offer other favorable attributes in that they (1) typically do not utilize rare earth materials, (2) operate at near atmospheric temperature and pressure conditions, (3) are feedstock flexible, and (4) are quick to start-up or

shut-down providing the ability to rapidly adapt to fluctuating feedstock pricing.^{74, 76} The three most common NTP techniques for CO₂ reduction include: dielectric barrier (DBD), microwave (MW), or gliding arc (GA) plasma discharges shown in Fig. 5.²¹

Accessible products from NTP reduction depend on both the reactor configuration (i.e., DBD, GA, MW) and type of feedstock(s). Introducing cofeeds of hydrogen containing compounds (e.g., H₂, CH₄, and H₂O) yields a mixture of hydrocarbon and oxygenated species.^{21, 74, 75, 77} Reported NTP-derived products are summarized in Table 2 with common metrics defined in Equations 3-6. Across the multiple NTP pathways and reactant combinations, CO and/or syngas yields are by far the highest, with individual oxygenates and hydrocarbons typically comprising < 3% without the addition of downstream packed-bed catalysts (e.g., zeolites, Al₂O₃, etc.).²¹

$$\text{Absolute Conversion: } X_{abs} = \frac{n_{in} - n_{out}}{n_{in}} \quad (3)$$

$$\text{Total Conversion: } X_{tot} = \sum_i \left(\frac{n_{i, inlets}}{\sum_i n_{i, inlets}} * X_{abs} \right) \quad (4)$$

$$\text{Energy Efficiency: } EE = \frac{X_i * \Delta H_{rxn}}{SEI} \quad (5)$$

$$\text{Specific Energy Input: } SEI = \frac{\text{Power Input}}{\text{Gas Flowrate}} = \left(\frac{\text{Joules}}{\text{Vol}} \right) \quad (6)$$

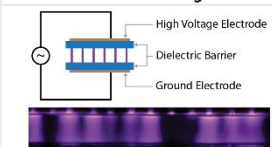
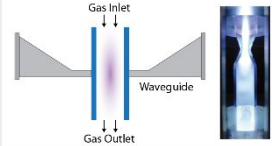
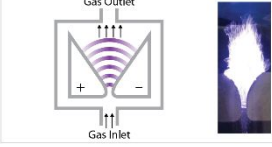
	ADVANTAGES	DISADVANTAGES
Dielectric Barrier Discharge 	<ul style="list-style-type: none"> Atmospheric pressure operation Low temperature / cold plasma Most mature technology Commercialized for ozone production, television sets 	<ul style="list-style-type: none"> Maximum energy efficiency ~15% Less efficient impact excitation dissociation mechanism
Microwave 	<ul style="list-style-type: none"> Demonstrated energy efficiencies > 40% More efficient stepwise vibrational excitation-dissociation mechanism 	<ul style="list-style-type: none"> Higher temperature / warm plasma Requires low pressures for operation (100-200 torr) Low technical maturity
Gliding Arc 	<ul style="list-style-type: none"> Atmospheric pressure operation More efficient stepwise vibrational excitation-dissociation mechanism 	<ul style="list-style-type: none"> Higher temperature / warm plasma Low conversion / gas residence time Low technical maturity

Figure 5: Common configurations for plasma-based CO₂ reduction and their advantages and disadvantages. Modified from^{21, 76, 77}.

Technical Challenges

Decoupling Energy Efficiency and Conversion

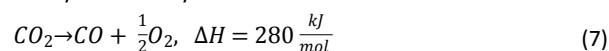
Energy efficiencies for NTP processes typically range from ≤ 15% in the case of DBD to ≤ 40-50% for MW/GA plasmas. A few notable MW studies dating back to the 1970s and 80s claim energy efficiencies of up to 90% under supersonic flow conditions; however, recent efforts to reproduce such high efficiencies have been unsuccessful.⁷⁸ Nevertheless, although MW/GA plasmas approach comparable energy efficiencies to other commercialized processes, peak energy efficiency values are observed only at low conversion (e.g., < 20%). Conversely, as conversion increases to in some cases over > 80%, corresponding energy efficiencies drop to < 5%.²¹

To advance NTP conversion technologies, a decoupling of conversion and energy efficiency is needed in order to increase both metrics simultaneously. With respect to energy efficiency, the current target is to at a minimum exceed the equilibrium energy efficiency limit for thermal CO₂ splitting of ~47% at ~70% conversion.²¹ Specific energy input (SEI, Eq. 6) is considered to be the most important factor impacting the reaction conversion and energy efficiency, being directly correlated to conversion and inversely correlated to energy efficiency for pure CO₂ reduction.²¹

To increase conversion without also sacrificing energy efficiency, the volume of treatable gas should be increased without increasing discharge power. Although higher discharge power positively impacts conversion by enhancing the electric field, density of electrons, and gas temperature within the plasma zone, it negatively impacts energy efficiency based on Equations 4 and 5 above.⁷⁹ Studies have shown some success at raising both metrics simultaneously by increasing gas pressure,⁸⁰ decreasing discharge gaps, decreasing the thickness of the dielectric barrier material, adding catalysts inside the plasma zone,⁸¹ or enlarging the discharge length.⁸² Raising both conversion and energy efficiency represents a fundamental long-term challenge.

Improving Hydrocarbon Yields and Product Selectivity:

NTP is an inherently non-selective approach due to radical-based chemistry. While not a challenge for pure CO₂ reduction as the products include only CO and O₂ (Eq. 7), the presence of a hydrogen source (e.g., H₂, CH₄, or H₂O) or inert species (e.g., N₂) significantly expands the possible reaction pathways. Yet, even in the presence of a hydrogen source, CO remains the dominant product when inlet CO₂ concentrations are > ca. 5%.^{21, 74} This observation is a direct consequence of the *in-situ* formation of O₂ (Eq. 7) which actively oxidizes hydrocarbon species into CO and H₂O contributing to low overall hydrocarbon yields.⁷⁴



To direct product selectivity towards higher value hydrocarbons, the effect of inert gas type (N₂, Ar, He), electrode material, dielectric barrier material, wall/gas temperature, applied frequency, discharge gap, specific energy input, CH₄:CO₂ ratio, and pressure, have been studied.²¹

Table 2: Summary of SOT plasma reduction metrics across common products

Species	Pathway	Conversion (%)	Selectivity (%)	Yield (%)	Energy Efficiency (%) ^a	CO ₂ Flowrate (mL / min)	Ref
CO	DBD ^b	26.0	100.0 ^c	26.0	23.0	200	83
CO	MW ^b	10.0	100.0 ^c	10.0	50.0	7500	76
CO	GA ^b	12.0	100.0 ^c	12.0	65.0	1700	21, 84
CH ₃ OH	DBD ^d	20.0 ^e	7.1	1.4	6.2	58 ^f	85
C ₂ H ₂	MW / Pulsed ^d	70.0 ^e	17.8	12.5	~8.5	80 ^g	86
CH ₂ O	DBD ^d	19.0 ^e	6.6	1.3	5.9	42 ^h	85
C ₂ H ₄	DBD / Pulsed ^d	25.1 ^e	63.7	16.0	14.1	17 ⁱ	87
C ₂ H ₆	DBD + HY Zeolite ^d	7.5 ^e	32.1	2.4	1.8	100 ^j	88
C ₂ H ₅ OH	DBD ^d	20.0 ^e	12.1	2.4	6.2	58 ^f	85
CH ₃ COOH	DBD ^d	20.0 ^e	7.2	1.4	6.2	58 ^f	85
C ₃ H ₆	DBD ^d	61.3 ^e	2.1	1.3	2.2	50 ^k	86
C ₃ H ₈	DBD ^d	18.3 ^e	8.9	1.6	5.7	20 ^l	85
C ₃ H ₇ OH	DBD ^d	20.0 ^e	1.7	0.3	6.2	58 ^f	85

a: Calculated based of Equation 5

b: Pure CO₂ decomposition

c: Only carbon containing product

d: CO₂ + CH₄ dry reforming reaction

e: Reflects total conversion for CO₂ + CH₄ mixture (Eq. 3)

f: Total flowrate 90 mL/min. 1.8:CO₂:CH₄

g: 200 mL/min total. ~1.5CH₄:CO₂

h: Total flowrate 90 mL/min 1.1 CH₄:CO₂

i: Total flowrate 100 mL/min. 6:1 CH₄:CO₂

j: Total flowrate 200 mL/min. 1:1 CH₄:CO₂

k: Total flowrate 150 mL/min. 2:1 CH₄:CO₂

l: Total flowrate 90 mL/min 3.4 CH₄:CO₂

The conditions found most favoring the formation of hydrocarbons and oxygenates include lower reaction temperatures (473-673 K),⁸⁹ lower applied power,⁹⁰ higher pressure,⁹⁰ and higher CH₄/CO₂ ratios.^{74, 91} However, even under optimized conditions, reported yields to hydrocarbons were on the order of only a few percent (Table 2).^{21, 89, 92}

Outside of modifying the reaction parameters, one of the most effective means to control product selectivity is a hybrid NTP route incorporating packed-bed heterogeneous catalysts. By combining plasma with heterogeneous catalysts, unique synergies are theoretically possible whereby CO₂ can be activated by plasma under near room temperature conditions and selectively recombined on the catalyst surface to yield desired products.²¹ Common catalysts include zeolites,^{86, 88, 92, 93} metal oxides,^{81, 89, 94-97} and ceramics.⁹⁸ In general, C₂-C₄ hydrocarbon selectivity improved with zeolite catalysts,^{86, 92} highlighted by a selectivity to C₄ hydrocarbons up to 52.1% using Zeolite HY by Zhang and co-workers.⁸⁸ Yet, despite some initial successes in forming higher-hydrocarbons, the overall yields and energy efficiencies for synthesizing non-syngas species remains low. Potential paths forward include development of plasma-specific catalysts with improved thermal stability allowing for combination with MW/GA plasmas which can leverage the more efficient reaction mechanisms.

Process Scale Up and Associated Hazards

The combination of high *in-situ* concentrations of O₂ along with other flammable species (e.g., CO, H₂, CH₄) and high-temperature ignition sources (e.g., plasma filaments) creates the risk of an explosive atmosphere. While lab-scale studies are generally regarded as low risk where volumes are small and conversions are low, the risk significantly increases with operation at the pilot and commercial scales. Risk mitigation may necessitate costly capital investments and higher operating expenses to ensure safe operation.⁹⁹ Common engineering controls based on cofeeding diluent gases (e.g., N₂, He,

Ar) comes with several drawbacks in that it can lead to containment formation (e.g., NO_x), increasing the cost of downstream separations and recycle and lowering process energy efficiency as input energy is lost to impact-excitation ionization of the spectator diluent gases rather than CO₂.⁹⁹ Research is needed for the development of *in-situ* separation methods that can cheaply and selectively remove O₂ from the process while having a minimal impact on process costs.

Direct Bioelectrochemical

Overview

Whereas abiotic electrochemical systems rely on metal-catalyzed reactions to reduce CO₂, reactions can also be catalyzed using microorganisms, either oxidatively on the anode or reductively on the cathode.¹⁰⁰ For the purposes of CO₂ reduction, the most common configuration involves an abiotic anode for OER paired with a biocathode inoculated with anaerobic microorganisms as shown in Fig. 6. However, as in the case of direct electrochemical reduction, abiotic or biotic oxidation of organics is also possible on the anode side to reduce overall cell voltage.^{52, 101} While still early stage R&D, microbial electrosynthesis (MES) conversion strategies show the potential for an array of favorable attributes; specifically (1) low energy input (low overpotential) needed to activate CO₂ reduction, (2) high selectivity to coupled carbon products with minimal side reactions, (3) mild operating conditions, and (4) inherent regenerative properties of the biocatalyst.¹⁰²

Microorganisms 'fix' carbon in coupled and non-coupled products at up to ~99% selectivity determined by one of the seven established metabolic reduction cycles: Calvin-Benson-Bassham, reductive TCA, reductive Acetyl-CoA (Wood-Ljungdahl), 3-Hydroxypropionate (3HP), Dicarboxylate 4-Hydroxybutyrate (4HB), 3-Hydroxypropionate 4-Hydroxybutyrate (3HP/4HB), or the recently proposed reductive glycine pathway.¹⁰²⁻¹⁰⁴ Currently, microorganisms known to accept

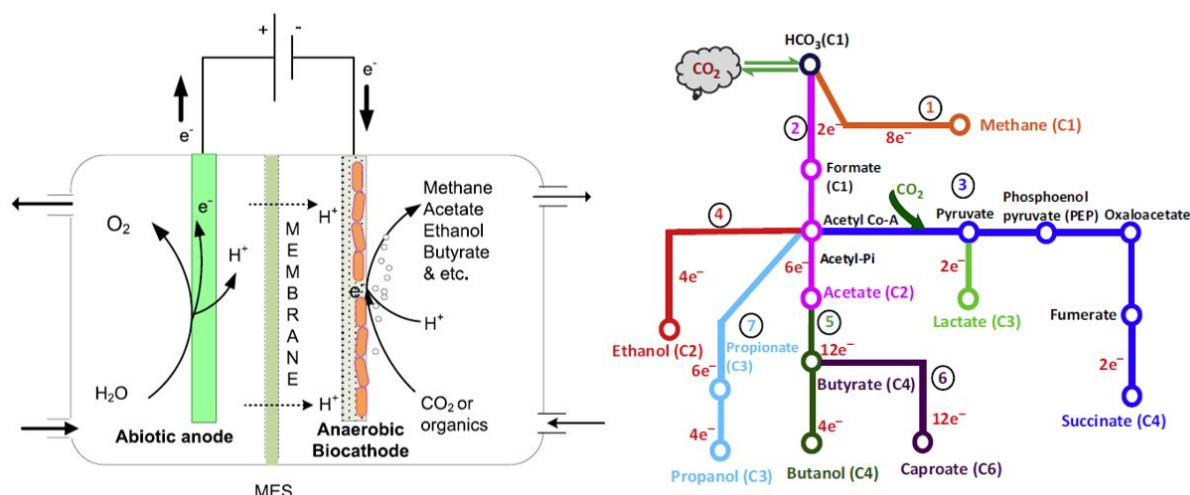


Figure 6: Conceptual representation of a microbial electrosynthesis cell with an abiotic anode and the Wood-Ljungdahl CO_2 fixation pathway. Reproduced with permission from 102, 105

Table 3: C_1 - C_3 Products accessible via direct bioelectrochemical reduction ranked by partial current density.

Species	#e ⁻	Std. Reduction Potential vs. SHE@ pH 7 (V) ^a	FE (%)	η (mV) ^b	j_{partial} (mA/cm ²)	ϵ (%) ^a	Ref
Acetate	8	-0.32	99	820	19.8	65.1	106
Methane	8	-0.24	70	1060	0.86	33.5	107
Ethanol	12	-0.33	11.6	485	0.12	7.1	108
Isopropanol	18	-0.31	21.8	647	0.11	12.2	109
Formate	2	-0.41	4.1	21	n.d.	3.2	110
Propionate	14	-0.30	n.d.	n.d.	n.d.	-	111

a: See Table S5 in supporting information for calculations.

b: Cathodic overpotential.

both synthesis gas (CO_2 , CO , H_2) and electrons are limited to anaerobic methanogenic and/or acetogenic species which have evolved to synthesize products exclusively through the Wood-Ljungdahl (WL) pathway.

Shown in Fig. 6, a variety of products are accessible through CO_2 fixation and the WL pathway including simple C_1 species up through C_6 . Although the catalog of electroactive bacteria capable of performing MES has expanded from the initial discovery of *Sporomusa ovata* in 2010 to include other pure and mixture cultures such as *C. ljungdahlii*, *M. thermoacetica*, and others, homoacetogens have been most extensively evaluated to date, in part due to their tolerance to a wide range of operating conditions and substrates.¹⁰² As such, acetate remains by far the most dominant product reported for pure cultures, demonstrating the highest-to-date production rate of 1330 g / m² d using a high surface area multi-wall carbon nanotube reticulated vitreous carbon cathode.¹⁰⁶ However, it should be stressed that an overemphasis solely on rate and the propensity to extrapolate lab-scale kinetic data can obscure other major technical hurdles such as product dilution and scalability, which remain as key uncertainties in deployment of such technology. Besides acetate, other reported products observed during MES include: H_2 , methane, formate, ethanol, propionate, butanol, butyrate, and 2-Oxobutyrate.¹¹² In Table 3, C_1 – C_3 MES products and the reported SOT metrics are provided.

Technical Challenges

Elucidating the Fundamental Electron Transfer Mechanism:

The flow of energy (i.e., electrons to and between electroactive microorganisms) within MES systems is poorly understood, representing a major fundamental barrier to optimization and development. Current understanding of extracellular electron transfer between the surface of an electrode to a neighboring microorganism is largely based on electron-donating (exoelectrogenic) species *Geobacter sulfurreducens* and *Shewanella oneidensis* str. MR-1²⁰ and it is unclear if the same mechanism(s) hold true for electron-accepting (electrotrophic) pathways. In fact, some recent studies suggest the mechanism could be entirely different.¹¹⁰ One of the greatest questions, and an area of active debate, is the feasibility of direct electron transfer (DIET) and possible role of H_2 formation. Outside of a few notable studies,¹¹³ most MES studies involving the reduction of CO_2 have been reported at potentials more negative than the H_2 evolution potential (-0.414 V vs. SHE)²⁰ implying the formation of H_2 was thermodynamically favorable.¹⁰² It has been argued that studies which suggest the presence of a DIET mechanism (i.e., not H_2 -mediated) simply based on failure to detect free H_2 gas, may actually go through a two-stage process whereby H_2 gas forms and subsequently (and immediately) acts as a mediator at the interface of the electrode and biofilm.

Considering the lack of fundamental understanding of inter- and intracellular electron transfer – which has been reported to vary based on operational parameters such as type of microorganism¹¹⁴ and applied potential¹¹² – more research is needed to characterize and understand microbial electron uptake, bifurcation, and transfer mechanism. For example, forward and reverse genetic approaches, coupled with systems level analyses, can further the fundamental understanding of mediators of electron flow, ultimately enabling targeted metabolic engineering strategies to optimize microbial electrosynthesis routes.

Increasing the Rate of CO₂ Reduction

Where abiotic alkaline water electrolyzers utilize current on the order of 200-400 mA/cm² and are limited only by mass transfer,²⁸ biological processing of electrons and carbon relies on membrane structure, enzyme kinetics, cofactor regeneration rates, among other variables which likely limit the utilization rate. To the authors' knowledge, no upper limit for electron utilization has been reported, but with SOT current densities ranging between 0.1 - 20 mA/cm² as shown in Table 3, a fundamental mismatch between electron availability and electron utilization within carbon fixation pathways may exist. In abiotic electrochemical processes, the most successful studies to date (and now commercial systems) capitalize on the benefits of gas diffusion electrodes in flow-cell configurations to increase local CO₂ concentrations, resulting in current densities now in excess of 750 mA/cm².³¹ Increasing current density towards the fundamental limit in MES systems may be attainable through similar utilization of GDE systems; however, few studies demonstrating a GDE-based MES process have been reported.^{108, 115} Developing biocompatible cathodes and GDEs which maximize surface area for cell coverage and are efficient in delivering reactants to the system requires further fundamental research and engineering.

Another challenge in pushing reduction rates lies in the stability of the biofilm. H₂ from competing HER along with CH₄ from mixed culture biofilms not only decreases faradaic efficiency and yield to higher-value multi-carbon species, but also can destabilize and cause detachment of microorganisms from the electrode surface.¹⁰² Microbe detachment fundamentally alters the reaction mechanism (i.e., direct vs. mediated electron transfer) and may limit the effectiveness of MES as microorganisms are removed from the electrode surface into the bulk phase.¹⁰² While CH₄ formation can be suppressed with chemical inhibitors such as sodium-2-bromoethanesulfonate (Na-BES) or alamethicin, routine inhibition can impact production costs as commercial inhibitor prices can be as high as \$175/g.^{111, 116} Conversely, raising cell voltage above -0.4 V vs. SHE is the only guaranteed means of HER cessation. However, to increase current densities (productivities), typically overpotentials will also increase, likely pushing cell voltages well inside the HER stability region. This implies that the evolution of H₂ and management of bubble formation on biofilm stability will require future study in any commercially scalable systems.

Raising Product Titrers and the Toxicity Limits of Microorganisms

With recent estimates suggesting the downstream purification and separation costs of biological processes accounting for up to 60% of the total production costs,¹¹⁷ the synthesis of end products with high titer and purity represents an ongoing challenge facing MES processes.¹⁰² Beyond a certain concentration of product, microbial metabolism can become inhibited, limiting titers in processes

without *in-situ* separation.¹⁰² For example, in the case of butanol only 1-2% accumulation can inhibit microorganism growth.¹¹⁸ As a result, separation cost can be burdensome. R&D efforts on synthesizing products with high faradaic efficiency along with high concentrations of targeted products will be needed for process economics. Further R&D is needed into both separation techniques and genetic engineering to tolerate higher titer of products.

Sustaining Microbial Communities During Intermittent Operation

Integration of renewable electricity with MES presents unique challenges due to the intermittent nature of renewable power.¹¹³ Intermittency has the potential to impact microbial community viability, composition, and productivity. Recent scientific findings have shown that microbial communities are resilient to short-term intermittencies, with near-complete rebound of MES community productivity following 64-hour power interruption.^{119, 120} However, long-term intermittency (>1 month) could be problematic. A shift of cathode communities from acetogenic to methanogenic has been discovered, and resultant productivity and end product profile were altered, despite maintaining electroactivity.¹²¹ Thus, strategies to rapidly reestablish and maintain target electroactive communities, such as selective enrichment, bioaugmentation, and applied external potential approaches, will likely be a critical consideration for deployment of MES at scale for sustained operability.^{122, 123}

Note that recent advances in enzymatic electrosynthesis present it as a potential means to bypass the intermittency challenges and mass transport and activation losses associated with whole cell microbial systems.¹²⁴ For instance, enzymatic electrosynthesis of formate has been achieved with coulombic efficiencies >90%.¹²⁵ Relatively low product yields, classical challenges associated with cell-free systems (such as enzyme and cofactor cost, cofactor regeneration, and long-term enzyme stability), and scalability are amongst the hurdles remaining to advance this technology.¹²⁶

Indirect Bioelectrochemical

Overview

The indirect non-photosynthetic microbial conversion of CO₂ represents a mature, and for some products, near market ready technology.¹²⁷ Indirect bioelectrochemical methods rely on the enzymes carbonic anhydrase and hydrogenase¹⁰³ for the conversion of CO₂ and H₂ respectively to a range of products including methane, acetate, alcohols, and other biofuels.¹²⁸⁻¹³² By separating the CO₂ conversion process into two or more distinct steps (i.e., H₂ formation followed by CO₂ reduction), several advantages are realized in comparison to the direct MES pathway. By isolating the microorganisms from the electricity source, possible complications related to exposure to electricity (e.g., protein denaturation, cell lysis), biofouling of the electrodes, and decoupling of electrolysis/fermentation temperature and pressure conditions can be avoided. Furthermore, the typically slower biological conversion process (Table 3) can be separated from the faster upstream production of the energy carrier (Table 1), which if stored in an intermediate reservoir (or transported), allows processes to selectively take advantage of fluctuating energy prices while maintaining continuous downstream conversion.¹³³

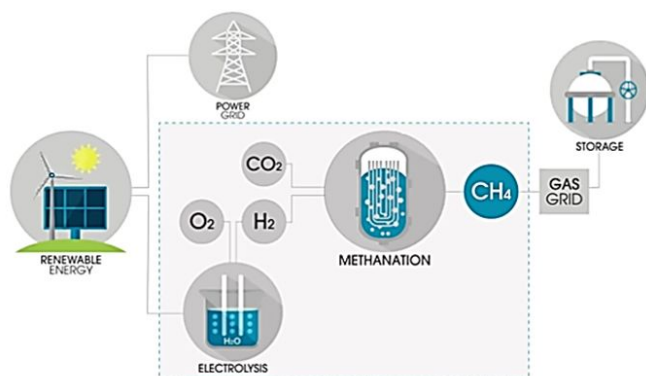


Figure 7: Overview of commercial power-to-gas process to produce methane from CO₂ and H₂. Reproduced from ¹²⁷.

Like the MES pathway, anaerobic methanogenic and acetogenic species are most commonly studied for CO₂ conversion, relying primarily on the Wood-Ljungdahl pathway. Thus, products observed in CO₂ + H₂ fermentation are again dominated by methane and acetate, with current SOT data for C₁-C₃ species shown in Table 4. There are a variety of other anaerobic and aerobic products accessible from CO₂ + H₂ (e.g., poly-hydroxybutyrate (PHB), botryococcene, methyl ketones) which are outside of our C₁-C₃ scope, though we acknowledge their promise in future CO₂ utilization.¹³⁴ From the perspective of the circular carbon economy, methanation or “power-to-gas” (P2G) technologies have recently gained attention commercially. Leveraging existing global infrastructure for natural gas transport, methanation of CO₂ via renewable energy represents an immediately deployable and potentially carbon-neutral pathway for the storage of excess electrical energy in chemical bonds. Highlighting the commercial readiness of this technology, in March 2015 MicrobEnergy demonstrated the first commercial-scale injection of biological methane upgraded from raw biogas and H₂ into the German national grid.¹³⁵ Additionally, in February 2014 Electrochaea launched an €6.7 million project in Copenhagen to construct the world’s largest commercial scale power-to-gas system consisting of a 1 MW alkaline electrolyzer paired with a local wastewater treatment plant to source CO₂ (Fig. 7).

Table 4: C₁-C₃ Products and Metrics for the Indirect Biochemical Pathway

Species	CO ₂ Conversion (%)	Selectivity (%)	Productivity (g/L day)	ε (%)	Ref
Methane	96 ^a	n.d.	206	n.d.	¹³⁶
Acetate	86	n.d.	149	56 ^b	¹³⁷
Isopropanol	n.d.	n.d.	0.098	31	¹³⁸

a: Y_{CH₄} in effluent gas

b: Calculated energy efficiency. (LHV products / LHV reactants)*0.7

Technical Challenges

Improving Mass Transfer to Overcome Low Reactant Solubility:

At 20 °C and 1 atm partial pressure, the solubility of H₂ and CO₂ in H₂O are 14.6 and 713 ppm respectively.^{139, 140} The low equilibrium concentration of reactants in solution limits fermentation productivity. Improving gas/liquid mass transfer (k_la) remains a challenge in reactor design and operating conditions. Over 95% of all bioreactors are continuous stirred-tank reactors (CSTR) due to high degree of mixing/agitation.¹⁴¹ The increased degree of mixing

achieved through manipulation of agitation rates, impeller design, sparger types, etc., does not come without cost, however. CSTRs also demonstrate poor volumetric power outputs (defined by power required per volume (P_R/V)).¹⁴² Therefore, the tradeoff between P_R/V and k_la must be evaluated to determine the most economically advantaged operating conditions.

Research is ongoing for the development of fixed-bed and hollow fiber membrane bioreactors that remove the need for active stirring (decreasing P_R/V) and minimize shear-induced microbial damage observed with CSTRs. In these systems, microorganisms can be affixed to different forms of scaffolding including solid particles, membranes, or fibers which increase the contact area for mass transport without the need for additional mechanical power input.¹⁴² Hollow fiber membranes offer additional advantages in that bubble-free gassing is made possible through the direct dissolution of gas into the liquid phase, making gas immediately available to cells leading to enhanced conversion efficiency.¹⁴² One of the greatest challenges to membrane utilization thus far is the limited lifespan and propensity to biofouling.¹⁴² Development of membranes which are more resilient to fatigue and fouling is needed. Additionally, genetic engineering of enzymatic processes for carbonic anhydrase and hydrogenase to over-express natural CO₂/H₂ concentration mechanisms is also an area of interest.^{103, 143}

Process Scale Up and Preserving System Anoxia:

To safely scale biological processes which may utilize a H₂ cofeed, keeping O₂ levels below the lower explosive limit will be critical to mitigating the risk of an explosive atmosphere. While at the lab-scale these issues are minimized, maintaining large scale system anoxia in commercial size processes can be costly and impact operating expenses (OPEX).¹⁰³ Concurrent research in both increasing the aero-tolerance^{103, 143} of anaerobic microorganisms as well as process design to engineer solutions for the possible accumulation of O₂ should be considered. Given the current success of modern anaerobic processes that utilize syngas,¹³⁴ this particular challenge does not represent a serious barrier to market adoption but rather is an opportunity for optimization and potential reduction of OPEX costs.

Indirect Thermochemical

Overview

Thermochemical pathways are of the oldest and most technologically mature routes for CO₂ conversion. Using a combination of heat, pressure, and inorganic catalysts, thermocatalytic hydrogenation of CO₂ offers a pathway to many hydrocarbon and oxygenated products, ranging in TRL from fully commercial to fundamental lab-scale R&D. At-scale processes are highlighted by recent demonstrations of methanol synthesis by Carbon Recycling International (CRI). Using locally sourced CO₂ and renewable H₂, CRI’s pilot plant produces methanol at the scale of ~5.5 kt/y making it the world’s largest CO₂ to methanol facility.¹⁴⁴ At the academic level, recent work has explored multi-functional catalysts for CO₂ hydrogenation with combined activity towards reverse water gas shift and syngas-derived product synthesis reactions (Fig. 8).¹⁴⁵ Strengths of thermochemical processes include: (1) high TRL, (2) availability of existing infrastructure and process know-how, and (3) the greatest range of accessible products amongst conversion pathways (e.g., FT, MOGD). In Table 5, common C₁-C₃ thermochemical-derived species and their SOT metrics are shown.

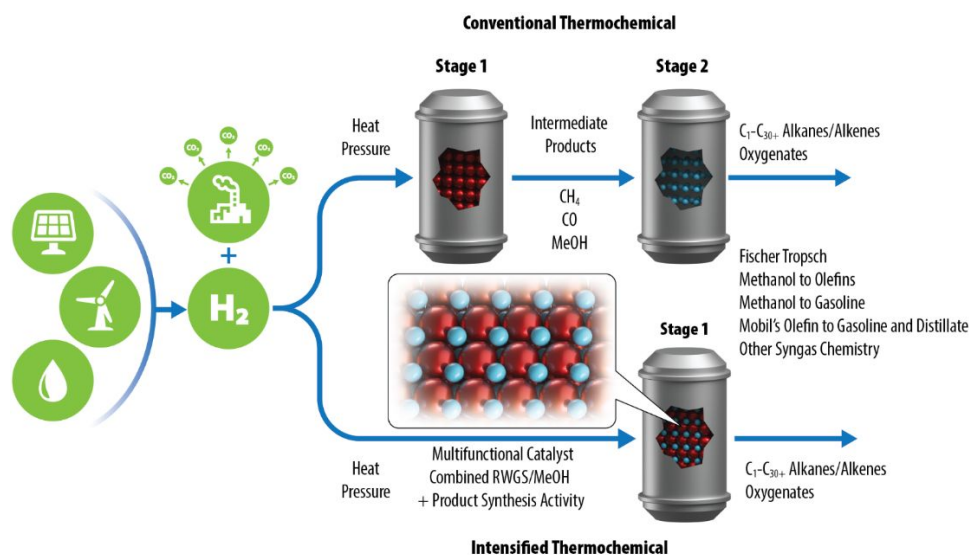
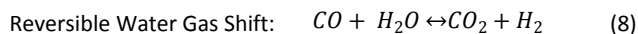


Figure 8: Process intensification through multifunctional catalyst for the one-step conversion of CO₂ to products.

Technical Challenges

Overcoming Equilibrium Conversion Limitations

Unlike other CO₂R pathways, most thermochemical reactions are reversible and are limited to some equilibrium CO₂ conversion at a given set of thermodynamic conditions. For example, in the reversible water gas shift reaction (Eq. 8), over normal reaction temperatures (e.g., 600 – 800 °C), single-pass conversion of CO₂ to CO is thermodynamically limited to around ~70%.¹⁴⁶ Compared to other reductive pathways which are not thermodynamically constrained in terms of equilibrium conversion (e.g., direct electrochemical), the conversion limitations of thermochemical conversion pathways lowers product yields and contributes to additional process cost stemming from downstream purification and recycle of unconverted species. Feeding excess H₂ or *in-situ* removal of products (e.g., H₂O) would help in raising equilibrium conversion based on Le Chatelier's principle; however, the economic tradeoff between conversion and additional process costs must be weighed. Further R&D into passive and/or low-cost gas separation operations would help to lessen the burden of downstream purification costs and potentially lead to improved single-pass yields.



Process Intensification:

Conventional thermochemical processes are conducted at large scales to maximize benefits associated with economies of scale. Fischer-Tropsch plants in particular leverage large-scale operations with modern facilities operating in the range of 34,000 – 160,000 bpd.¹⁴⁷ Although technologically mature at this massive scale (e.g., Sasol, South Africa), process intensification and downsizing to a scale compatible with distributed CO₂ sources is an area of active research. Multiple technical and engineering challenges related to the consolidation of process stages, heat management and integration, and low process throughputs must accordingly be addressed in order to economically scale down and intensify modern thermochemical processes. As one example, during CO₂/CO hydrogenation reactions, water is a common byproduct and sink for oxygen. For many heterogenous catalysts, water and hydroxyl formation are poisons which negatively impact conversion, hydrocarbon selectivity, and catalyst durability.^{148, 149} In traditional multi-stage processes, water is actively removed in-between stages to mitigate these challenges; however, in a shift towards process intensification and multifunctional catalysts that combine multiple synthesis steps, developing catalysts which can tolerate higher concentrations of water will be critical to minimizing deactivation.

Table 5: C₁-C₃ Products accessible via Indirect Thermochemical Pathway

Species	#e-	T (°C)	P (bar)	H ₂ :CO ₂	Space Velocity	CO ₂ Conversion (%) ^a	Selectivity (%)	Productivity (g / g _{cat} h)	ε (%) ^b	Ref
CO	2	650	n.d.	4:1	12,500 ^c	~70%	~100%	0.17	45 ^d	146, 150
Methanol	6	260	360	10:1	10,471 ^e	>95%	>98%	1.2	50-60	39, 46, 151
Methane	8	400	1	4:1	15,000 ^e	81%	99%	3.3	55	152, 153
DME	12	260	50	3:1	3,000 ^c	31%	73%	0.16	n.d.	154
Ethylene	12	400	15	3:1	12,000 ^c	~12	34%	0.08	n.d.	155
Propylene	18	400	15	3:1	12,000 ^c	~12	56%	0.13	n.d.	155

a: Max conversion dictated by thermodynamics depending on (T/P/H₂:CO₂)

b: Energy efficiency includes 0.7 multiplier to account for ε losses in electrolysis step.

c: mL / g_{cat} hr

d: Calculated from ref as LHV of CO produced over total heat + LHV H₂ added

e: 1/hr

Further, with most incumbent syngas-based thermochemical processes configured to utilize CO + H₂, development of “tandem catalysts” capable of facilitating multiple reactions in a single step with a CO₂ feedstock is needed.

If realized, process intensification presents the potential for more economical and environmentally benign CO₂-based processes,¹⁴⁵ with possible additional synergetic benefits in terms of heat integration (e.g., pairing endothermic/exothermic reactions) and shifting equilibrium conversions (e.g., *in-situ* consumption of products driving CO₂ conversion). Although efforts devoted to process scale down are ongoing and are being tested through commercial ventures like Velocys,¹⁵⁶ additional R&D is needed to further develop process intensification strategies.

Improving Product Selectivity:

Initial catalyst testing for the direct hydrogenation of CO₂ has primarily involved the most successful CO hydrogenation catalysts (e.g., Cu/ZnO/Al₂O₃, Fe₃O₄, Co/Al₂O₃).¹⁴⁵ However, due to the differences in surface binding properties of CO₂ and CO, specifically in the relative rates of adsorption and desorption, CO₂-based processes are prone to rapid hydrogenation to highly reduced species (e.g., CH₄) versus more desirable coupled carbon species such as olefins and gasoline range hydrocarbons.^{18, 145, 157} In Fig. 9, experimental Anderson-Schulz-Flory (ASF) product distributions for CO and CO₂ hydrogenation over Co/Al₂O₃ are reported by Visconti et al.¹⁵⁸ Experiments feeding CO/H₂ showed a typical ASF hydrocarbon distribution (i.e. carbon numbers ranging from 0-50) where experiments incorporating solely CO₂/H₂ were heavily weighted to CH₄ and terminated around n=6, highlighting the challenge in forming long-chain hydrocarbons.¹⁵⁸

To drive the selectivity of CO₂ hydrogenation away from C₁ species to coupled hydrocarbon products, recent reports have studied the addition of metal promoter molecules such as K, Mn, Na, and Cu.¹⁴⁵ Alkali and transition metal promoters were shown to have a positive effect in increasing CO₂ conversion¹⁵⁹⁻¹⁶¹, suppressing CH₄ formation¹⁵⁷, increasing hydrocarbon chain growth¹⁶², and modifying paraffin/olefin ratios^{159, 161}. Continued advancements in catalyst development to further increase activity for CO₂ activation while

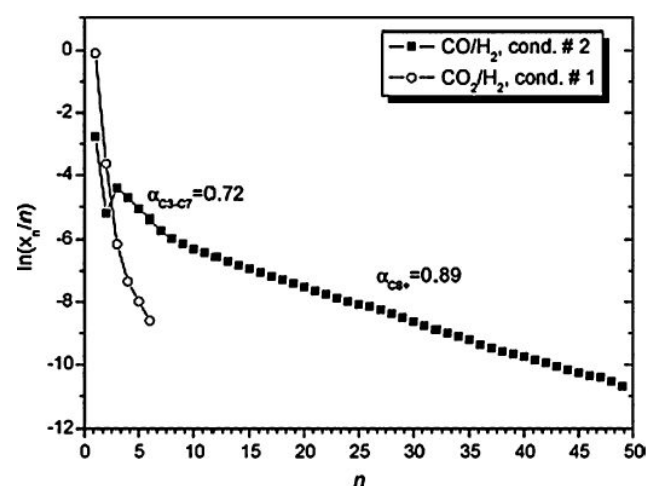


Figure 9: Anderson-Schulz-Flory (ASF) product distribution during CO and CO₂ hydrogenation over Co/Al₂O₃. Reproduced with permission from¹⁵⁸.

promoting high selectivity to longer chain hydrocarbon products are needed to drive down process separation costs and reach targeted products with high specificity.

Summary and Cross-Comparison of CO₂R Pathways

CO₂R is possible through at least five unique pathways ranging from inorganic electro- and thermocatalytic processes to biological approaches whereby microorganisms directly convert CO₂ within internal metabolic cycles. A summary of the major technical challenges, research needs, advantages, and limitations is shown in Fig. 10. In addition, a cross-comparison of the pathways, as discussed below, highlights several important intrinsic differences between these CO₂R pathways.

Thermodynamic Limits on Single-Pass Conversion

In the electrochemical, bioelectrochemical, and plasma pathways, single-pass CO₂ conversion can theoretically reach 98.6-100% with only small losses from cell reproduction.^{127, 163} By comparison, indirect thermochemical hydrogenation reactions are reversible and thermodynamically limited to an equilibrium conversion determined by temperature, pressure, and feedstock concentrations. Under industrially relevant reaction conditions, thermochemical CO₂ single-pass conversions typically range from ~27% to ~70% for methanol and CO, respectively.^{146, 164} These limits on CO₂ conversion lower product yields and drive up process cost associated with purification and recycle. Therefore, despite the high TRL of thermochemical pathways, limitations on equilibrium conversion may hinder their advancement and deployment, especially as the lower TRL pathways continue to advance. However, it should also be noted that productivity, which is typically highest in temperature thermochemical reactions, may help to offset the differences in purification/recycle costs.

Quantity and Quality of Products:

Within the scope of this work, a clear disparity exists in the quantity of products accessible between biological and non-biological routes. Amongst the non-biological pathways, direct electrochemical studies report over 20+ products, thermochemical routes can access numerous products via one-step FT and other established chemistries (e.g., direct methanol-to-olefins), and plasmas form 10+ species through radical-based chemistries. By comparison, biological utilization of CO₂ following the Wood-Ljungdahl pathway forms mostly methane, formate, acetate, and C₂-C₃ alcohols.¹⁰⁵ When considering the potential for future market disruption and utilization of CO₂, under the assumptions of this study, the direct electrochemical and indirect thermochemical routes offer access to the most high-volume, high-value CO₂R products. Further, many of the high-volume industrial chemicals are exclusive to non-biological routes such as CO, methanol, ethylene, and FT liquids. However, despite forming fewer overall C₁-C₃ products, biological routes possess a key advantage in terms of selectivity. Whereas electrochemical, plasma, and to a lesser degree thermochemical routes, suffer from poor selectivity to C₂+ products, microorganisms are specially adapted at forming carbon-carbon bonds with high selectivity within their internal metabolic pathways.

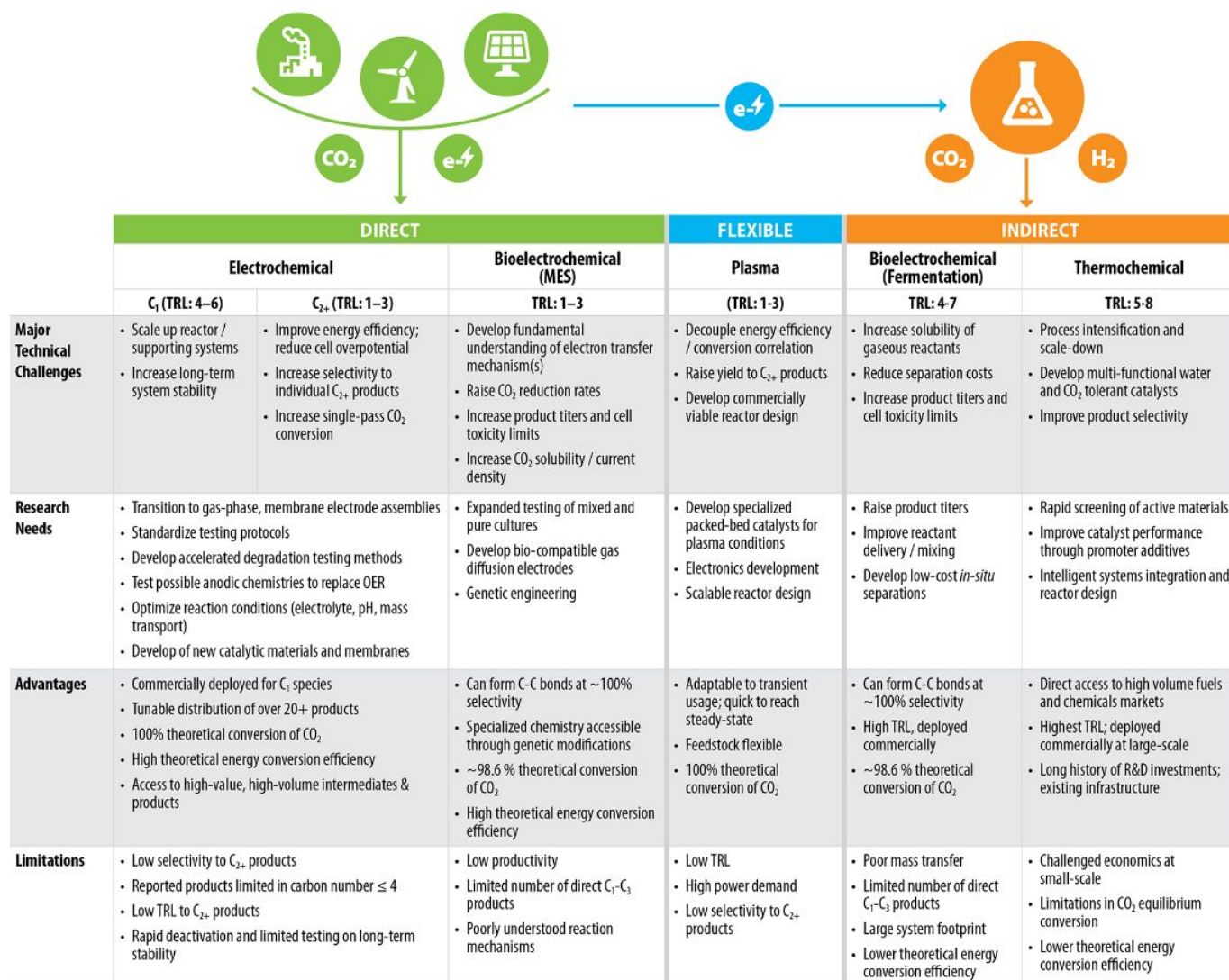


Figure 10: Summary of top technical barriers and areas for future research across CO₂R pathways.

Near-Term Opportunities and Technical Maturity

In comparing the relative TRL across the five CO₂R pathways shown in Fig. 10, the indirect conversion pathways are best positioned near-term for low-cost electricity utilization. Despite requiring additional steps for upstream H₂ generation, pre-commercial demonstrations of indirect CO₂R have confirmed the technical viability of these routes in the synthesis of several products (e.g., MeOH, CH₄, CO) at relevant scales.^{26, 144, 153} In general, the technical barriers facing indirect pathways are characterized by systems engineering and optimization challenges. Direct pathways are by comparison much lower TRL (1-6) and are in most cases limited to lab-scale testing, facing more fundamental science challenges with significantly longer time horizons. NTP and MES CO₂R pathways show the lowest TRL range of 1-3 and are expected to have the longest development timeline. The direct electrochemical pathway varies in TRL from 1-6 depending on the product formed. Specifically, the synthesis of select C₁ products over non-Cu electrodes has been demonstrated at comparably higher TRL (4-6) and is currently being tested commercially. However, the synthesis of C₂₊ products faces many challenges in the core conversion step as noted above with a longer anticipated timeline for development.

General Considerations for CO₂R

Sourcing CO₂

CO₂ sources span the range from the near-infinite atmospheric supply at ~415 ppm to concentrated streams released from biorefineries and ammonia synthesis plants. Characteristic values of concentration, emitted volume, impurities, and capture costs are provided in Table 6. Sources with the most concentrated streams require the least intensive cleanup and processing (e.g., fertilizer and bioethanol plants) and show the lowest first-of-a-kind (FOAK) CCS costs at 20 – 25 \$/tonne CO₂. By comparison, costs from dilute and low purity sources such as power plant flue gases range from 40 – 100 \$/tonne CO₂.

While the cost and quality of CO₂ play a role in determining the economic viability and location of CO₂R processes, factors such as supply volumes, access to low-cost and renewable (depending upon local and national policies) electricity, and proximity to downstream processing infrastructure should also be considered. In Fig. 11 an overlay of these factors across the United States shows that often

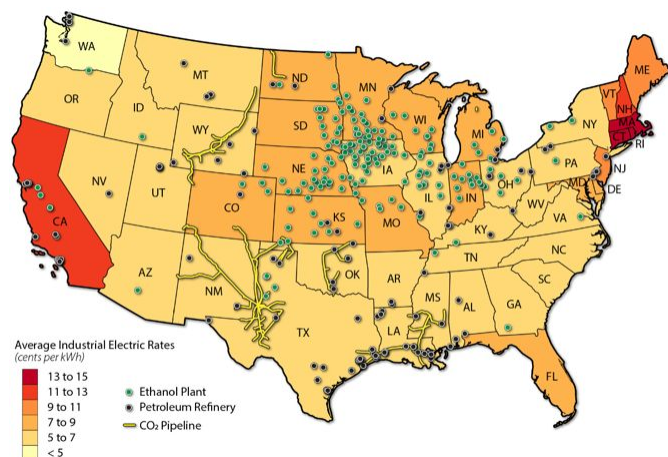


Figure 11: Overlay of US CO₂ pipeline infrastructure, ethanol facilities, and petroleum refining with average industrial electricity rates per by state. Electricity rates and ethanol plant locations based on 2017 data.¹⁶⁵⁻¹⁶⁷ Petroleum refinery locations based on 2018 data.¹⁶⁷

the least expensive CO₂ sources (i.e., bioethanol refinery waste gases) are mostly isolated from CO₂ transportation infrastructure and centralized refining, while also, in general, occurring in regions with higher industrial electric rates. Consequently, future CO₂R developments may likely require: (1) dedicated upgrading or processing infrastructure at each site and (2) evaluation of the economic tradeoff between CO₂ and electricity costs. In the absence of investments for new pipelines or other infrastructure to facilitate transport to a central processing type facility, CO₂R processes will need to overcome the challenges associated with distributed scale processing at each CO₂ site.

One means of simultaneously addressing the issues of supply, location, and scalability is direct air capture (DAC) of CO₂. Although currently the most expensive pathway for capture by a wide margin with estimates ranging from ~\$400/tonne to \$1000/tonne,¹⁶⁸ DAC is source agnostic and can be located virtually anywhere, taking advantage of cheap land, low-cost electricity, and potential co-location with processing infrastructure. Furthermore, although CO₂ point sources comprise a significant portion of global emissions, approximately 40% of all emitted CO₂ comes from non-point sources such as transportation which can only be captured using a DAC-type

approach.¹⁶⁹ With current at-scale designs capable of capturing 22-23 tons CO₂/m²/year based on frontal area, early estimates suggest that DAC technologies may be able to capture up to 1 million tons of CO₂ per year per 1 square kilometer footprint.^{48, 170} Further R&D for CO₂ capture technologies specifically surrounding tandem capture-convert processes, new sorbents, and reducing the energy intensity of regeneration could greatly accelerate and expand deployment of future CO₂R processes.

Product Separation and Purification:

Independent of the targeted product, a commonality shared by CO₂R pathways is the need for downstream separation and purification. Even mature pathways which achieve near 100% selectivity to a specific product will require separation from unconverted reactants (e.g., H₂O, CO₂, H₂) or from the parent electrolyte (if applicable). Thus, when evaluating specific reductive pathways or products, it is necessary to not only consider the challenges and costs associated with synthesis, but also the costs and technical challenges related to separations. While exact separations costs depend on a range of operational parameters, previous estimates for separating dilute mixtures based on Sherwood plots suggest the costs of separating liquid/organic products can be 6-10x more expensive than gaseous species.^{171, 172} While liquid/organic products often command a higher market price, which can to a degree offset higher separations costs, the additional costs must be weighed upfront. Clearly, the costs of separating a gaseous product from an aqueous electrolyte will be significantly different than the separation of ethanol where the cost of separation can easily exceed its value as a fuel.

Evaluation of CO₂R Products

With at least 5 unique conversion pathways and over 20+ accessible C₁-C₃ species, selecting promising product-pathway combinations for a future circular carbon economy is a complex question. As discussed, CO₂R is motivated by several forces, including economic potential from low-cost feedstocks, mitigation of CO₂ emissions through utilization, and the storage of otherwise curtailed renewable electricity. Below we evaluate each of these areas, along with a ranking of the relative ease of formation, to present the most advantaged products in each category.

Table 6: Quality of CO₂ from various sources.

Source	CO ₂ Concentration (%) ^a	Est. # Plants (2017) ^b	Average Volume CO ₂ Emitted (MMT / plant y) ^b	Common Impurities ^a	Capture Cost (\$/ton) ^c
Ethanol Fermentation	99	210	0.22	EtOH, MeOH, H ₂ S, H ₂ O, C ₂ H ₆ S	20-22
Ammonia Synthesis	>95	29	1.14	NH ₃ , H ₂ , CO, H ₂ O	24-25
Natural Gas Wells	90-100	N/A	N/A	N ₂ , CH ₄ , C ₂ H ₆ , C ₃ H ₈ , trace HCs	20-22
Coal-Fired Flue Gas	10-12	324	3.73	NO _x , SO _x , CO, O, N, Hg, As, Se	46-97
Gas-Fired Flue Gas	3-6	1128	0.47	NO _x , SO _x , CO, O, N, Hg, As, Se	43-89
Atmospheric CO ₂	415ppm	-	-	N ₂ , O ₂	400-1000

a:¹⁷³

b:^{166, 174}

c:^{168, 175}

Ease of Formation

Ease of formation reflects the relative technical feasibility of synthesizing a product and herein is qualitatively determined based on four factors: (1) rate of formation / partial current density, (2) faradaic efficiency / selectivity, (3) energy efficiency, and (4) current TRL. Across each of the four categories, a value of low, medium, or high was assigned (see Fig. 12 footnotes). In evaluating the products accessible across the five pathways, six products stand out as top performers in these areas: CO, ethylene, formate, methane, acetate, and methanol as shown in Fig. 12. CO, ethylene, and formate were selected as each has been synthesized electrochemically with partial current densities > 100 mA/cm² at a faradaic efficiency > 60%. Amongst direct bioelectrochemical pathways, acetate was selected as SOT current densities are over 6x higher than the next closest species and acetate can be formed at near 100% faradaic efficiency. For the indirect pathways, methanol and methane were selected based on high current TRL (i.e., low *technical* barriers to formation) and high achievable rates of formation. Based on these metrics, products are ranked in terms of ease of formation: CO, methanol > methane > formate > ethylene, acetate.

Market Forces

While overcoming fundamental technical challenges will accelerate the market-readiness of CO₂R pathways, the underlying product-market fit plays a critical role in determining the rate of deployment. In Table 7, the market price (\$/kg), global production in MMT/y, and potential impact on CO₂ utilization are reported, where available, for 22 reported C₁-C₃ products. Unless otherwise noted, listed market price reflects average values in 2016\$USD in the United States from 2014 - 2018. Of the species where data was accessible, all but one product shows a current market price on the order of 0.1 – 1.0 2016\$USD / kilogram. The one exception is electrochemically derived carbon nanotubes (CNT) which are priced two orders of magnitude higher than the next most valuable product at \$110.2 / kg. Recognizing that products vary in terms of electron intensity, market prices normalized by the number of electrons required for reduction are also reported. Note for thermochemical and bioelectrochemical processes which indirectly utilize electrons, we assume that each mol of H₂ consumes 2 e⁻. After normalization, three species stand out relative to baseline; CNTs at two orders of magnitude higher price, formic acid at one order of magnitude higher price, and methane at an order of magnitude lower price. It should be noted that methane price is based on US natural gas price and does not consider geographical differences and/or the impact of renewable natural gas markets which can command a higher price depending on the level of subsidies. The two above average performing species may represent initial entry points for FOAK processes. CNTs in particular show compelling economics as recent reports estimate electrochemical production costs at ~\$660/ton compared to the current market price of > \$100,000/ton for small scale chemical vapor deposition processes.^{176, 177} However, due to the relatively small demand for CNTs and formic acid at 0.003 and 0.6 MMT/y respectively, it is unlikely that these species would offer a long-term pathway for CO₂R NOAK (Nth-of-a-kind) facilities due to rapid market saturation. Nevertheless, formic acid is also considered as a feedstock for biological and thermochemical pathways and may be further converted in to products with much larger markets, such as fuels, solvents, plastic monomers, and food-grade protein.¹³³

Species	Rate of Formation ^a	Selectivity ^b	Energy Efficiency ^c	Current TRL ^d
Carbon Monoxide	High	High	High	High
Ethylene	High	Medium	Low	Low
Formate	Medium	High	Medium	Low
Methane	High	High	Medium	High
Acetate	Low	High	Medium	Low
Methanol	High	High	High	High

^a High: >200 mA/cm² (or commercial TC), Medium: 200 >/>100 mA/cm², Low: <100 mA/m²

^b High: >80%, Medium 80% > FE > 60%, Low: < 60%

^c High: >60%, Medium 60% > EE > 40%, Low: < 40%

^d High: Operated at TRL > 6, Medium: Operated TRL 4-6, Low: Operated TRL 1-3

Figure 12: Qualitative evaluation of product ease of formation.

Potential for CO₂ Utilization

In addition to market price, the CO₂ volume required to meet the current global demand of a given product and the potential impact on global CO₂ utilization was also considered. Specifically, in 2017 the US Environmental Protection Agency (EPA) estimated a total of 324 domestic coal-fired power plants ≥ 0.0025 MMT/y CO_{2e}, emitting a total of 1.21 billion metric tons of CO_{2e} or 1.02 MMT of carbon per plant per year.¹⁶⁶ A similar analysis can be done for other point sources such as gas-fired power generation and bioethanol production, showing on average 87-97% less emissions than that of coal fired power leading to only 0.13 and 0.06 MMT/y of carbon emitted per site, respectively.^{166, 174} Using these figures and the C₁-C₃ market data, the global production of a species in terms of carbon equivalent (i.e., total mass of carbon / year) can be viewed in terms of equivalent number of point sources required to satisfy the demand (assuming that 100% of all CO₂ emitted from each source is converted to products).

From this analysis, the total global market of 11 of the 22 possible products could be saturated by the carbon produced by one average coal-fired power plant in the United States. Note, for species where no data was accessible, it is assumed the market is under the 1.02 MMT/y carbon threshold. A complete analysis of market size in terms of carbon equivalent versus the number of theoretical point sources required is depicted in Fig. 13. Despite showing the lowest normalized market price, CH₄ has an order of magnitude higher global production compared to the next largest product (CO, syngas). Thus, from the perspective of the circular utilization of CO₂, CH₄ presents the most compelling option, especially when considering the existing infrastructure which may be leveraged. Alternatively, smaller FOAK installations or processes that involve the production of low volume products (e.g., formic acid and CNT) may be more suitable for pairing with non-coal fired or distributed CO₂ generation.

Table 7: Market data on C₁-C₃ products

Species	#e-	Pathway	US Market Price (\$/kg) ^a	\$/e- req. (x10 ³) ^b	Global Production (MMT/y)	CO ₂ e (MMT CO ₂ /y)	Equiv. # Coal Plants ^c	Ref
Carbon Monoxide	2	EC, TC	0.18	2.6	150	236	63	4, 178
Formic Acid	2	EC, TC	0.66 ^d	15.2	0.6	0.60	< 1	4, 179
Carbon Nanotubes	4	EC	110.2	331.0	0.003 ^e	0.01	< 1	177, 180
Methanol	6	EC, TC	0.35	1.9	91.8 ^f	126	34	179
Methane ^g	8	EC, TC, BC	0.15	0.3	2336	6410	1715	181, 182
Acetic Acid	8	EC, BC	0.61	4.6	14.3	21	6	179
Ethylene Glycol	10	EC	0.93	5.8	28.3 ^h	40	11	178, 179
Acetaldehyde	10	EC	1.42	6.3	0.9 ^e	1.8	< 1	178
Dimethyl Ether	12	TC	0.65 ⁱ	2.5	3.7	7.1	2	179, 183
Ethanol	12	EC, TC, BC	0.52	2.0	89.6	171	46	179
Ethylene	12	EC, TC, BC	0.71	1.7	156	490	134	179
Acetone	16	EC	1.00	3.4	6.8 ^j	15	4	178, 179
Propionaldehyde	16	EC	1.6 ^k	5.8	0.6 ^l	1.4	< 1	178
Propylene	18	TC	1.07	2.5	117	367	100	179
1-Propanol	18	EC	1.43	4.8	0.2	0.4	< 1	4
Isopropanol	18	BC	1.07	3.6	1.9 ^f	4.2	1	178, 179
Oxalate	2	EC	n.d.	n.d.	n.d.	n.d.	n.d.	-
Glyoxal	6	EC	n.d.	n.d.	n.d.	n.d.	n.d.	-
Glycolaldehyde	8	EC	n.d.	n.d.	n.d.	n.d.	n.d.	-
Hydroxyacetone	14	EC	n.d.	n.d.	n.d.	n.d.	n.d.	-
Propionate	14	BC	n.d.	n.d.	n.d.	n.d.	n.d.	-
Allyl Alcohol	16	EC	n.d.	n.d.	n.d.	n.d.	n.d.	-

a: 2014-2018 average price in United States unless otherwise noted

b: Normalized price calculated based on mole of electrons required per mole of product.

c: United States EPA 2017 emissions data.¹⁶⁶ 324 total operating coal fired power plants in U.S. producing a total of 3.30 GT/y of CO₂ yielding average of 1.02 MMT/y carbon per plant.

d: Average of 2014 and 2016 price.

e: 2015 global consumption

f: Average 2017-2018 global consumption

g: Assumes natural gas price and market size

h: Average 2016-2017 global consumption

i: Average Chinese spot price in 2014-2018 converted to USD

j: 2016 global consumption

k: Average Western European price in 2008

l: 2017 global consumption

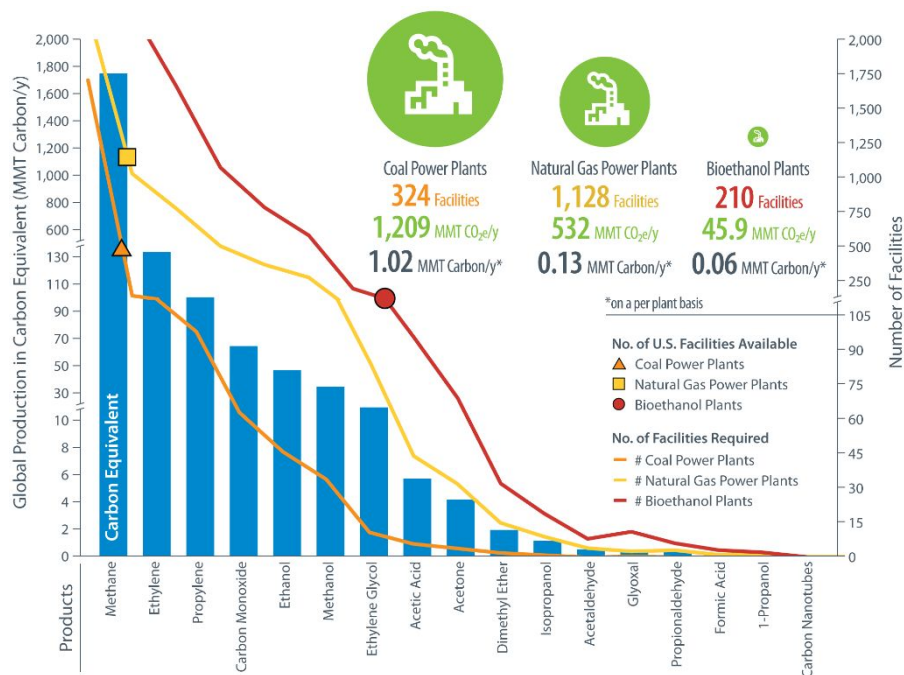


Figure 63: Global production in Carbon Equivalent of 22 CO₂R derived C₁-C₃ species combined with the number of coal power, natural gas power, and bioethanol plants needed to satisfy that global demand assuming 100% CO₂ conversion.

Table 8: Efficiency in converting electrical energy to chemical energy. Modified from ³⁹.

Species	HHV (kJ / mol)	e ⁻ Req. (-)	E _{c,i} (kJ / C)	Energy Stored rel. H ₂ (%)
Glyoxal	860.9	6	143	100.3%
H ₂	286	2	143	100.0%
CO	283	2	142	99.0%
Glycolaldehyde	1036.2	8	130	90.6%
Formic Acid	253.8	2	127	88.7%
DME	1460	12	122	85.1%
Oxalate (acid)	242.9	2	121	84.9%
Methanol	726	6	121	84.6%
Hydroxyacetone	1667.9	14	119	83.3%
Ethylene Glycol	1191	10	119	83.3%
Ethylene	1411	12	118	82.2%
Acetaldehyde	1167	10	117	81.6%
Allyl Alcohol	1852.8	16	116	81.0%
Propylene	2058	18	114	80.0%
Ethanol	1368	12	114	79.7%
Acetone	1821	16	114	79.6%
Propionaldehyde	1816.5	16	114	79.4%
Propanol	2021.3	18	112	78.5%
Isopropanol	2007	18	112	78.0%
Methane	891	8	111	77.9%
Acetate	875	8	109	76.5%
Propionate	1527.3	14	109	76.3%

Energy Storage

The storage of electricity during off-peak hours or times of oversupply across daily and/or seasonal cycles is one advantage of CO₂R processes over conventional petrochemical synthesis. To evaluate and rank the relative performance of products as an energy storage medium, Martin et al.³⁹ proposed comparing the number of electrons required for a reduction reaction against the amount of chemical energy contained within each species (i.e., the higher heating value (HHV)), which would thereby reveal the efficiency between electrical energy input and chemical energy stored. In Table 8 the energy storage capacities in kJ per coulomb (kJ / C) of the direct CO₂R products (i.e., electrochemical and MES) considered within this report (excluding CNTs) are shown relative to H₂ as a baseline. As shown, the energy stored in chemical bonds normalized by electrons required for reduction is, in general, inversely proportional to the number of electrons consumed. Therefore, from the perspective of energy storage, species that require the transfer of only a few electrons (e.g., 2-6), demonstrate high faradaic efficiency/selectivity, and allow for easy recovery of energy should be targeted. In comparing SOT faradaic efficiencies in Tables 1 and 3 with the energy conversion data in Table 8, noteworthy products include CO (99.9% FE, 142 kJ / C) and formate (90% FE, 127 kJ / C). Interestingly, although glyoxal and glycolaldehyde show promising energy storage values at 143 and 130 kJ / C respectively, the reported faradaic efficiencies of each species are low, limiting their practicality as an energy storage product.

Conclusions

The utilization of CO₂ and shift towards a sustainable and circular carbon economy is fraught with many technical challenges. Herein five CO₂R pathways were evaluated under state-of-technology conditions, specifically emphasizing the advantages and disadvantages and R&D needs, serving as a first-of-a-kind guide for the near- and long-term development of these diverse CO₂R technologies. An evaluation of the technical barriers across the five CO₂R pathways has shown that indirect routes (thermochemical and bioelectrochemical) offer the most technically feasible near-term opportunities for utilization of CO₂, representing immediately deployable pathways to high-value and relatively high-volume products. Yet, despite their near-term promise, indirect processes face inherent challenges with respect to lower equilibrium conversion (thermochemical) and a limited C₁-C₃ product distribution (biochemical), potentially hindering their long-term viability. In cross comparing direct and indirect pathways, emerging technologies such as the direct electrochemical pathway show tremendous long-term promise and can theoretically overcome these limitations, yet currently face numerous technical barriers preventing near-term market adoption. If the top technical challenges and R&D needs described within can be addressed and paired with accompanying advancements to CO₂ capture and purification, it will solidify a bright future for CO₂R and help lead the transition to a more sustainable circular carbon economy.

To complement the analysis of CO₂R technologies, 22 C₁-C₃ species accessible via CO₂R were evaluated in terms of ease of formation, market potential, CO₂ utilization potential, and energy storage capacity. The products with the highest ease of formation were CO and methanol based on relative TRL and conversion metrics, representing immediately deployable entry points for CO₂R. With respect to near-term profitability, electrochemically derived carbon nanotubes were shown to command the highest normalized selling price in terms of \$/electron transferred and the greatest reduction in synthesis cost relative to incumbent methods. From the perspective of CO₂ utilization, the global production of over half of the studied 22 products were sufficiently small that the global supply could be fulfilled by the CO₂ emitted from one average coal-fired power plant. However, at current market levels the combined impact from the 22 near-term C₁-C₃ products could offset up to 78% of the 10.1 GT CO₂ emitted annually from global coal power, showing the tremendous potential for utilization of CO₂. Further, as these C₁-C₃ products are combusted, degraded, or are incinerated at their end of life, the CO₂ re-released into the environment can be captured and converted once again, fostering a circular carbon economy. The products with the greatest potential to utilize CO₂ were CH₄, CO (via syngas), and C₂H₄. For the efficient conversion of electrical energy to chemical bond formation in seasonal or off-peak energy storage applications, CO and formic acid represent the top near-term targets based on SOT conditions. These results underscore that no one product is likely to dominate in CO₂R, but rather it will be a concerted effort between multiple product and pathway combinations.

Conflicts of interest

There are no conflicts to declare.

Acknowledgements

This work was authored by the National Renewable Energy Laboratory, operated by Alliance for Sustainable Energy, LLC, for the U.S. Department of Energy (DOE) under Contract No. DE-AC36-08GO28308. Funding provided by the U.S. Department of Energy Office of Energy Efficiency and Renewable Energy Bioenergy Technologies Office. The views expressed in the article do not necessarily represent the views of the DOE or the U.S. Government. The U.S. Government retains and the publisher, by accepting the article for publication, acknowledges that the U.S. Government retains a nonexclusive, paid-up, irrevocable, worldwide license to publish or reproduce the published form of this work, or allow others to do so, for U.S. Government purposes.

Authors would like to acknowledge and thank all subject matter experts who agreed to be interviewed and shared their expertise during the writing of this perspective. Authors would also like to acknowledge Anelia Milbrandt and Billy Roberts from the Strategic Energy Analysis Center for their assistance in preparing Fig.11. Authors also acknowledge Abhijit Dutta for assistance in conducting expert interviews informing the analysis as well as Jesse Hensley for providing a thorough review of the manuscript.

Notes and references

1. C. Le Quéré, R. M. Andrew, P. Friedlingstein, S. Sitch, J. Pongratz, A. C. Manning, J. I. Korsbakken, G. P. Peters, J. G. Canadell, R. B. Jackson, T. A. Boden, P. P. Tans, O. D. Andrews, V. K. Arora, D. C. E. Bakker, L. Barbero, M. Becker, R. A. Betts, L. Bopp, F. Chevallier, L. P. Chini, P. Ciais, C. E. Cosca, J. Cross, K. Currie, T. Gasser, I. Harris, J. Hauck, V. Haverd, R. A. Houghton, C. W. Hunt, G. Hurtt, T. Ilyina, A. K. Jain, E. Kato, M. Kautz, R. F. Keeling, K. Klein Goldewijk, A. Körtzinger, P. Landschützer, N. Lefèvre, A. Lenton, S. Lienert, I. Lima, D. Lombardozi, N. Metz, F. Millero, P. M. S. Monteiro, D. R. Munro, J. E. M. S. Nabel, S.-i. Nakaoka, Y. Nojiri, X. A. Padín, A. Peregon, B. Pfeil, D. Pierrot, B. Poulter, G. Rehder, J. Reimer, C. Rödenbeck, J. Schwinger, R. Séférian, I. Skjelvan, B. D. Stocker, H. Tian, B. Tilbrook, I. T. van der Laan-Luijckx, G. R. van der Werf, S. van Heuven, N. Viovy, N. Vuichard, A. P. Walker, A. J. Watson, A. J. Wiltshire, S. Zaehle and D. Zhu, *Earth System Science Data Discussions*, 2017, DOI: 10.5194/essd-2017-123, 1-79.
2. Global CCS Institute, 2018 Global Status Report, <https://www.globalccsinstitute.com/resources/global-status-report/download/>, (accessed 5/16/2019).
3. *Gaseous Carbon Waste Streams Utilization: Status and Research Needs (2019)*, National Academy of Sciences, 2019.
4. M. Jouny, W. Luc and F. Jiao, *Industrial & Engineering Chemistry Research*, 2018, **57**, 2165-2177.
5. H. Yang, C. Zhang, P. Gao, H. Wang, X. Li, L. Zhong, W. Wei and Y. Sun, *Catalysis Science & Technology*, 2017, **7**, 4580-4598.
6. A. Katelhon, R. Meys, S. Deutz, S. Suh and A. Bardow, *Proc Natl Acad Sci U S A*, 2019, **116**, 11187-11194.
7. International Energy Agency, Iron and Steel: Tracking Clean Energy Progress, <https://www.iea.org/tcep/industry/steel/>, (accessed 5/15/2019).
8. K. Kermeli, E. Worrell, W. Graus and M. Corsten, *Energy Efficiency and Cost Saving Opportunities for Ammonia and Nitrogenous Fertilizer Production*, 2017.
9. E. Worrell, D. Phylipsen, D. Einstien and M. Nathan, *Energy Use and Energy Intensity of the U.S. Chemical Industry*, 2000.
10. International Renewable Energy Agency, *Renewable Power Generation Costs in 2017*, 2018.
11. Renewable Capacity Highlights: 2019, <https://www.irena.org/publications/2019/Mar/Renewable-Capacity-Statistics-2019>, (accessed 5/23/2019).
12. C. Brandstät, G. Brunekreeft and K. Jahnke, *Energy Policy*, 2011, **39**, 3732-3740.
13. Renewables 2018: Market Analysis and Forecast from 2018-2023, <https://www.iea.org/renewables2018/>, (accessed 5/16/2019).
14. Global Roadmap for Implementing CO₂ Utilization, <https://www.globalco2initiative.org/opportunity/>, (accessed 6/6/2019).
15. *Impacts, Risks, and Adaptation in the United States: Fourth National Climate Assessment*, U.S. Global Change Research Program, Washington, DC, USA, 2018.
16. *Climate Change 2014: Mitigation of Climate Change. Working Group III Contribution to the Fifth Assessment Report of the Intergovernmental Panel on Climate Change*, Intergovernmental Panel on Climate Change, 2014.
17. P. De Luna, C. Hahn, D. Higgins, S. A. Jaffer, T. F. Jaramillo and E. H. Sargent, *Science*, 2019, **364**.
18. W. Wang, S. Wang, X. Ma and J. Gong, *Chem Soc Rev*, 2011, **40**, 3703-3727.
19. W. Zhang, Y. Hu, L. Ma, G. Zhu, Y. Wang, X. Xue, R. Chen, S. Yang and Z. Jin, *Adv Sci (Weinh)*, 2018, **5**, 1700275.
20. K. Rabaey and R. A. Rozendal, *Nat Rev Microbiol*, 2010, **8**, 706-716.
21. R. Snoeckx and A. Bogaerts, *Chem Soc Rev*, 2017, **46**, 5805-5863.

22. L.-C. Weng, A. T. Bell and A. Z. Weber, *Energy & Environmental Science*, 2019.
23. K. P. Kuhl, E. R. Cave, D. N. Abram and T. F. Jaramillo, *Energy & Environmental Science*, 2012, **5**, 7050.
24. K. U. D. Calvino, A. B. Laursen, K. M. K. Yap, T. A. Goetjen, S. Hwang, N. Murali, B. Mejia-Sosa, A. Lubarski, K. M. Teeluck, E. S. Hall, E. Garfunkel, M. Greenblatt and G. C. Dismukes, *Energy & Environmental Science*, 2018, **11**, 2550-2559.
25. Y. Hori, K. Kikuchi and S. Suzuki, *The Chemical Society of Japan*, 1985, 1695-1698.
26. C. Mittal, C. Hadsbjerg and P. Blennow, *Chemical Engineering World*, 2017.
27. C. Duan, R. Kee, H. Zhu, N. Sullivan, L. Zhu, L. Bian, D. Jennings and R. O'Hayre, *Nature Energy*, 2019, **4**, 230-240.
28. M. Carmo, D. L. Fritz, J. Mergel and D. Stolten, *International Journal of Hydrogen Energy*, 2013, **38**, 4901-4934.
29. C. Ainscough, D. Peterson and E. Miller, *Hydrogen Production Cost from PEM Electrolysis*, https://www.hydrogen.energy.gov/pdfs/14004_h2_production_cost_pem_electrolysis.pdf, (accessed 5/14/2019).
30. L. Ye, M. Zhang, P. Huang, G. Guo, M. Hong, C. Li, J. T. Irvine and K. Xie, *Nat Commun*, 2017, **8**, 14785.
31. C. T. Dinh, T. Burdyny, M. G. Kibria, A. Seifitokaldani, C. M. Gabardo, F. P. Garcia de Arquer, A. Kiani, J. P. Edwards, P. De Luna, O. S. Bushuyev, C. Zou, R. Quintero-Bermudez, Y. Pang, D. Sinton and E. H. Sargent, *Science*, 2018, **360**, 783-787.
32. H. Wu, Z. Li, D. Ji, Y. Liu, L. Li, D. Yuan, Z. Zhang, J. Ren, M. Lefler, B. Wang and S. Licht, *Carbon*, 2016, **106**, 208-217.
33. S. Ma, R. Luo, J. I. Gold, A. Z. Yu, B. Kim and P. J. A. Kenis, *Journal of Materials Chemistry A*, 2016, **4**, 8573-8578.
34. D. Kopljär, A. Inan, P. Vindayer, N. Wagner and E. Klemm, *Journal of Applied Electrochemistry*, 2014, **44**, 1107-1116.
35. T. T. H. Hoang, S. Verma, S. Ma, T. T. Fister, J. Timoshenko, A. I. Frenkel, P. J. A. Kenis and A. A. Gewirth, *J Am Chem Soc*, 2018, **140**, 5791-5797.
36. Z. Twardowski, *United States Pat. 9267212B2*, 2016.
37. T.-T. Zhuang, Z.-Q. Liang, A. Seifitokaldani, Y. Li, P. De Luna, T. Burdyny, F. Che, F. Meng, Y. Min, R. Quintero-Bermudez, C. T. Dinh, Y. Pang, M. Zhong, B. Zhang, J. Li, P.-N. Chen, X.-L. Zheng, H. Liang, W.-N. Ge, B.-J. Ye, D. Sinton, S.-H. Yu and E. H. Sargent, *Nature Catalysis*, 2018, **1**, 421-428.
38. K. Manthiram, B. J. Beberwyck and A. P. Alivisatos, *Journal of the American Chemical Society*, 2014, **136**, 13319-13325.
39. A. J. Martín, G. O. Larrazábal and J. Pérez-Ramírez, *Green Chemistry*, 2015, **17**, 5114-5130.
40. H. Zhou, F. Yu, J. Sun, R. He, S. Chen, C. W. Chu and Z. Ren, *Proc Natl Acad Sci U S A*, 2017, **114**, 5607-5611.
41. N. Macauley, D. D. Papadias, J. Fairweather, D. Spornjak, D. Langlois, R. Ahluwalia, K. L. More, R. Mukundan and R. L. Borup, *Journal of The Electrochemical Society*, 2018, **165**, F3148-F3160.
42. R. L. Borup, J. R. Davey, F. H. Garzon, D. L. Wood and M. A. Inbody, *Journal of Power Sources*, 2006, **163**, 76-81.
43. S. Maass, F. Finsterwalder, G. Frank, R. Hartmann and C. Merten, *Journal of Power Sources*, 2008, **176**, 444-451.
44. C. C. McCrory, S. Jung, I. M. Ferrer, S. M. Chatman, J. C. Peters and T. F. Jaramillo, *J Am Chem Soc*, 2015, **137**, 4347-4357.
45. S. P. S. Badwal, S. Giddey and F. T. Ciacchi, *Ionics*, 2006, **12**, 7-14.
46. M. Aresta, A. Dibenedetto and A. Angelini, *Philos Trans A Math Phys Eng Sci*, 2013, **371**, 20120111.
47. M. A. Pellow, C. J. M. Emmott, C. J. Barnhart and S. M. Benson, *Energy & Environmental Science*, 2015, **8**, 1938-1952.
48. W. A. Smith, T. Burdyny, D. A. Vermaas and H. Geerlings, *Joule*, 2019, **3**, 1822-1834.
49. T. Burdyny and W. A. Smith, *Energy & Environmental Science*, 2019.
50. D. A. Torelli, S. A. Francis, J. C. Crompton, A. Javier, J. R. Thompson, B. S. Brunschwig, M. P. Soriaga and N. S. Lewis, *ACS Catalysis*, 2016, **6**, 2100-2104.
51. D. Raciti, K. J. Livi and C. Wang, *Nano Lett*, 2015, **15**, 6829-6835.
52. S. Verma, S. Lu and P. J. A. Kenis, *Nature Energy*, 2019.
53. O. G. Sánchez, Y. Y. Birdja, M. Bulut, J. Vaes, T. Breugelmans and D. Pant, *Current Opinion in Green and Sustainable Chemistry*, 2019, **16**, 47-56.
54. C. Coutanceau and S. Baranton, *Wiley Interdisciplinary Reviews: Energy and Environment*, 2016, **5**, 388-400.
55. S. Rousseau, C. Coutanceau, C. Lamy and J. M. Léger, *Journal of Power Sources*, 2006, **158**, 18-24.
56. A. S. Varela, W. Ju, T. Reier and P. Strasser, *ACS Catalysis*, 2016, **6**, 2136-2144.
57. E. B. Cole, P. S. Lakkuraju, D. M. Rampulla, A. J. Morris, E. Abelev and A. B. Bocarsly, *Journal of the American Chemical Society*, 2010, **132**, 11539-11551.
58. C. W. Li and M. W. Kanan, *J Am Chem Soc*, 2012, **134**, 7231-7234.
59. R. Reske, H. Mistry, F. Beharfarid, B. Roldan Cuenya and P. Strasser, *J Am Chem Soc*, 2014, **136**, 6978-6986.
60. W. J. Durand, A. A. Peterson, F. Studt, F. Abild-Pedersen and J. K. Nørskov, *Surface Science*, 2011, **605**, 1354-1359.
61. D. Kim, J. Resasco, Y. Yu, A. M. Asiri and P. Yang, *Nat Commun*, 2014, **5**, 4948.
62. Y. Hori, H. Wakebe, T. Tsukamoto and O. Koga, *Electrochimica Acta*, 1994, **39**, 1833-1839.
63. Y. Lum, B. Yue, P. Lobaccaro, A. T. Bell and J. W. Ager, *The Journal of Physical Chemistry C*, 2017, **121**, 14191-14203.
64. C. W. Li, J. Ciston and M. W. Kanan, *Nature*, 2014, **508**, 504-507.
65. X. Feng, K. Jiang, S. Fan and M. W. Kanan, *ACS Cent Sci*, 2016, **2**, 169-174.
66. Y. Hori, in *Modern Aspects of Electrochemistry*, eds. C. G. Vayenas, R. E. White and M. E. Gamboa-Aldeco, Springer, New York, 2008, vol. 42, pp. 89-189.
67. Y. Hori, I. Takahashi, O. Koga and N. Hoshi, *Journal of Molecular Catalysis A: Chemical*, 2003, **199**, 39-47.
68. A. D. Handoko, C. W. Ong, Y. Huang, Z. G. Lee, L. Lin, G. B. Panetti and B. S. Yeo, *The Journal of Physical Chemistry C*, 2016, **120**, 20058-20067.
69. Y. Hori, R. Takahashi, Y. Yoshinami and A. Murata, *J. Phys. Chem. B*, 1997, **101**, 7075-7081.
70. D. Ren, Y. Deng, A. D. Handoko, C. S. Chen, S. Malkhandi and B. S. Yeo, *ACS Catalysis*, 2015, **5**, 2814-2821.
71. N. Gupta, M. Gattrell and B. MacDougall, *Journal of Applied Electrochemistry*, 2005, **36**, 161-172.
72. D. M. Weekes, D. A. Salvatore, A. Reyes, A. Huang and C. P. Berlinguette, *Acc Chem Res*, 2018, **51**, 910-918.
73. R. Goldston and P. Rutherford, *Introduction to Plasma Physics*, CRC Press, Boca Raton, 1995.
74. W. Wang, R. Snoeckx, X. Zhang, M. S. Cha and A. Bogaerts, *The Journal of Physical Chemistry C*, 2018, **122**, 8704-8723.
75. B. Ashford and X. Tu, *Current Opinion in Green and Sustainable Chemistry*, 2017, **3**, 45-49.
76. W. Bongers, H. Bouwmeester, B. Wolf, F. Peeters, S. Welzel, D. van den Bekerom, N. den Harder, A. Goede, M. Graswinckel, P. W. Groen, J. Kopecki, M. Leins, G. van Rooij, A. Schulz, M. Walker and R. van de Sanden, *Plasma Processes and Polymers*, 2017, **14**.
77. X. Tao, M. Bai, X. Li, H. Long, S. Shang, Y. Yin and X. Dai, *Progress in Energy and Combustion Science*, 2011, **37**, 113-124.
78. G. J. van Rooij, D. C. van den Bekerom, N. den Harder, T. Minea, G. Berden, W. A. Bongers, R. Engeln, M. F. Graswinckel, E. Zoethout and M. C. van de Sanden, *Faraday Discuss*, 2015, **183**, 233-248.
79. H. J. Gallon, X. Tu and J. C. Whitehead, *Plasma Processes and Polymers*, 2012, **9**, 90-97.
80. A. Lebouvier, S. A. Iwarere, P. d'Argenlieu, D. Ramjugernath and L. Fulcheri, *Energy & Fuels*, 2013, **27**, 2712-2722.
81. K. Van Laer and A. Bogaerts, *Energy Technology*, 2015, **3**, 1038-1044.
82. D. Mei and X. Tu, *Journal of CO2 Utilization*, 2017, **19**, 68-78.
83. A. Ozkan, A. Bogaerts and F. Reniers, *Journal of Physics D: Applied Physics*, 2017, **50**.
84. S. C. Kim, M. S. Lim and Y. N. Chun, *Plasma Chemistry and Plasma Processing*, 2013, **34**, 125-143.

85. J.-J. Zou, Y.-p. Zhang, C.-j. Liu, Y. Li and B. Eliasson, *Plasma Chemistry and Plasma Processing*, 2003, **23**, 69-82.
86. B. Eliasson, C.-j. Liu and U. Kogelschatz, *Industrial & Engineering Chemistry Research*, 2000, **39**, 1221-1227.
87. S. L. Yao, F. Ouyang, A. Nakayama, E. Suzuki, M. Okumoto and A. Mizuno, *Energy & Fuels*, 2000, **14**, 910-914.
88. K. Zhang, B. Eliasson and U. Kogelschatz, *Industrial & Engineering Chemistry Research*, 2002, **41**, 1462-1468.
89. V. Goujard, J.-M. Tatibouët and C. Batiot-Dupeyrat, *Applied Catalysis A: General*, 2009, **353**, 228-235.
90. C.-j. Liu, B. Xue, B. Eliasson, F. He, Y. Li and G.-h. Xu, *Plasma Chemistry and Plasma Processing*, 2001, **21**, 301-310.
91. C.-j. Liu, G.-h. Xu and T. Wang, *Fuel Processing Technology*, 1999, **58**, 119-134.
92. T. Jiang, Y. Li, C.-j. Liu, G.-h. Xu, B. Eliasson and B. Xue, *Catalysis Today*, 2002, **72**, 229-235.
93. K. Zhang, U. Kogelschatz and B. Eliasson, *Energy & Fuels*, 2001, **15**, 395-402.
94. I. Michielsen, Y. Uytendhouwen, J. Pype, B. Michielsen, J. Mertens, F. Reniers, V. Meynen and A. Bogaerts, *Chemical Engineering Journal*, 2017, **326**, 477-488.
95. X. Duan, Z. Hu, Y. Li and B. Wang, *AIChE Journal*, 2015, **61**, 898-903.
96. Q. Wang, B.-H. Yan, Y. Jin and Y. Cheng, *Energy & Fuels*, 2009, **23**, 4196-4201.
97. A.-J. Zhang, A.-M. Zhu, J. Guo, Y. Xu and C. Shi, *Chemical Engineering Journal*, 2010, **156**, 601-606.
98. M. Kraus, B. Eliasson, U. Kogelschatz and A. Wokaun, *Physical Chemistry Chemical Physics*, 2001, **3**, 294-300.
99. R. Snoeckx, A. Ozkan, F. Reniers and A. Bogaerts, *ChemSusChem*, 2017, **10**, 409-424.
100. G. Zhen, X. Lu, G. Kumar, P. Bakonyi, K. Xu and Y. Zhao, *Progress in Energy and Combustion Science*, 2017, **63**, 119-145.
101. L. Lu, Z. Huang, G. H. Rau and Z. J. Ren, *Environ Sci Technol*, 2015, **49**, 8193-8201.
102. S. Bajracharya, S. Srikanth, G. Mohanakrishna, R. Zacharia, D. P. Strik and D. Pant, *Journal of Power Sources*, 2017, **356**, 256-273.
103. A. S. Hawkins, P. M. McTernan, H. Lian, R. M. Kelly and M. W. Adams, *Curr Opin Biotechnol*, 2013, **24**, 376-384.
104. I. A. Figueroa, T. P. Barnum, P. Y. Somasekar, C. I. Carlstrom, A. L. Engelbrekton and J. D. Coates, *Proc Natl Acad Sci U S A*, 2018, **115**, E92-E101.
105. S. V. Mohan, J. A. Modestra, K. Amulya, S. K. Butti and G. Velvizhi, *Trends Biotechnology*, 2016, **34**, 506-519.
106. L. Jourdin, S. Freguia, V. Flexer and J. Keller, *Environ Sci Technol*, 2016, **50**, 1982-1989.
107. Y. Jiang, M. Su, Y. Zhang, G. Zhan, Y. Tao and D. Li, *International Journal of Hydrogen Energy*, 2013, **38**, 3497-3502.
108. S. Srikanth, D. Singh, K. Vanbroekhoven, D. Pant, M. Kumar, S. K. Puri and S. S. V. Ramakumar, *Bioresour Technol*, 2018, **265**, 45-51.
109. J. B. A. Arends, S. A. Patil, H. Roume and K. Rabaey, *Journal of CO2 Utilization*, 2017, **20**, 141-149.
110. K. P. Nevin, S. A. Hensley, A. E. Franks, Z. M. Summers, J. Ou, T. L. Woodard, O. L. Snoeyenbos-West and D. R. Lovley, *Appl Environ Microbiol*, 2011, **77**, 2882-2886.
111. C. W. Marshall, D. E. Ross, E. B. Fichot, R. S. Norman and H. D. May, *Environ Sci Technol*, 2013, **47**, 6023-6029.
112. N. Aryal, F. Ammam, S. A. Patil and D. Pant, *Green Chemistry*, 2017, **19**, 5748-5760.
113. K. P. Nevin, T. L. Woodard, A. E. Franks, Z. M. Summers and D. R. Lovley, *MBio*, 2010, **1**.
114. A. Sydow, T. Krieg, F. Mayer, J. Schrader and D. Holtmann, *Appl Microbiol Biotechnol*, 2014, **98**, 8481-8495.
115. S. Bajracharya, K. Vanbroekhoven, C. J. Buisman, D. Pant and D. P. Strik, *Environ Sci Pollut Res Int*, 2016, **23**, 22292-22308.
116. X. Zhu, M. Siegert, M. D. Yates and B. E. Logan, *Appl Environ Microbiol*, 2015, **81**, 3863-3868.
117. I. Bechthold, K. Bretz, S. Kabasci, R. Kopitzky and A. Springer, *Chemical Engineering & Technology*, 2008, **31**, 647-654.
118. E. P. Knoshaug and M. Zhang, *Appl Biochem Biotechnol*, 2009, **153**, 13-20.
119. M. del Pilar Anzola Rojas, R. Mateos, A. Sotres, M. Zaiat, E. R. Gonzalez, A. Escapa, H. De Wever and D. Pant, *Energy Conversion and Management*, 2018, **177**, 272-279.
120. M. Del Pilar Anzola Rojas, M. Zaiat, E. R. Gonzalez, H. De Wever and D. Pant, *Bioresour Technol*, 2018, **266**, 203-210.
121. R. Mateos, A. Escapa, M. I. San-Martín, H. De Wever, A. Sotres and D. Pant, *Journal of Energy Chemistry*, 2020, **41**, 3-6.
122. S. A. Patil, J. B. Arends, I. Vanwonterghem, J. van Meerbergen, K. Guo, G. W. Tyson and K. Rabaey, *Environ Sci Technol*, 2015, **49**, 8833-8843.
123. D. A. Jadhav, A. D. Chendake, A. Schievano and D. Pant, *Bioresour Technol*, 2019, **277**, 148-156.
124. P. Chiranjeevi, M. Bulut, T. Breugelmanns, S. A. Patil and D. Pant, *Current Opinion in Green and Sustainable Chemistry*, 2019, **16**, 65-70.
125. M. Lienemann, J. S. Deutzmann, R. D. Milton, M. Sahin and A. M. Spormann, *Bioresour Technol*, 2018, **254**, 278-283.
126. Q. M. Dudley, A. S. Karim and M. C. Jewett, *Biotechnol J*, 2015, **10**, 69-82.
127. Electrochaea, <http://www.electrochaea.com/technology/>, (accessed 03/12/2018).
128. H. Li, P. H. Opgenorth, D. G. Wernick, S. Rogers, T. Y. Wu, W. Higashide, P. Malati, Y. X. Huo, K. M. Cho and J. C. Liao, *Science*, 2012, **335**, 1596.
129. M. Szuhaj, N. Acs, R. Tengolics, A. Bodor, G. Rakhely, K. L. Kovacs and Z. Bagi, *Biotechnol Biofuels*, 2016, **9**, 102.
130. M. Kopke, C. Held, S. Hujer, H. Liesegang, A. Wiezer, A. Wollherr, A. Ehrenreich, W. Liebl, G. Gottschalk and P. Durre, *Proc Natl Acad Sci U S A*, 2010, **107**, 13087-13092.
131. B. F. Pfeleger, *Proc Natl Acad Sci U S A*, 2016, **113**, 3717-3719.
132. C. T. Chen and J. C. Liao, *FEMS Microbiol Lett*, 2016, **363**, fnw020.
133. O. Yishai, S. N. Lindner, J. Gonzalez de la Cruz, H. Tenenboim and A. Bar-Even, *Curr Opin Chem Biol*, 2016, **35**, 1-9.
134. P. Durre and B. J. Eikmanns, *Curr Opin Biotechnol*, 2015, **35**, 63-72.
135. M. Bailera, P. Lisbona, L. M. Romeo and S. Espatolero, *Renewable and Sustainable Energy Reviews*, 2017, **69**, 292-312.
136. J.-P. Peillex, M.-L. Fardeau and J.-P. Belaich, *Biomass*, 1990, **21**, 315-321.
137. T. Morinaga and N. Kawada, *Journal of Biotechnology*, 1990, **14**, 187-194.
138. C. Liu, B. C. Colon, M. Ziesack, P. A. Silver and D. G. Nocera, *Science*, 2016, **352**, 1210-1213.
139. J. J. Carroll, J. D. Slupsky and A. E. Mather, *Journal of Physical and Chemical Reference Data*, 1991, **20**, 1201-1209.
140. NIST, Solubility Data Series: Volume 5/6 Hydrogen and Deuterium, <https://srdata.nist.gov/solubility/IUPAC/SDS-5-6/SDS-5-6.pdf>, (accessed 03/12/2018).
141. J. Nielsen, J. Villadsen and G. Liden, *Bioreaction Engineering Principles*, Springer, New York, 2011.
142. S. Rittmann, A. Seifert and C. Herwig, *Crit Rev Biotechnol*, 2015, **35**, 141-151.
143. A. S. Hawkins, Y. Han, H. Lian, A. J. Loder, A. L. Menon, I. J. Iwuchukwu, M. Keller, T. T. Leuko, M. W. W. Adams and R. M. Kelly, *ACS Catalysis*, 2011, **1**, 1043-1050.
144. The George Olah Renewable Methanol Plant, <https://www.carbonrecycling.is/george-olah>, (accessed 6/6/2019).
145. H. Yang, J. J. Kaczur, S. D. Sajjad and R. I. Masel, *Journal of CO2 Utilization*, 2017, **20**, 208-217.
146. L. Pastor-Pérez, F. Baibars, E. Le Sache, H. Arellano-García, S. Gu and T. R. Reina, *Journal of CO2 Utilization*, 2017, **21**, 423-428.
147. D. Leckel, *Energy & Fuels*, 2009, **23**, 2342-2358.
148. O. Martin and J. Pérez-Ramírez, *Catalysis Science & Technology*, 2013, **3**.
149. A. K. Dalai and B. H. Davis, *Applied Catalysis A: General*, 2008, **348**, 1-15.

150. Y. A. Daza, R. A. Kent, M. M. Yung and J. N. Kuhn, *Industrial & Engineering Chemistry Research*, 2014, **53**, 5828-5837.
151. A. Bansode and A. Urakawa, *Journal of Catalysis*, 2014, **309**, 66-70.
152. B. Mutz, H. W. P. Carvalho, S. Mangold, W. Kleist and J.-D. Grunwaldt, *Journal of Catalysis*, 2015, **327**, 48-53.
153. M. Götz, J. Lefebvre, F. Mörs, A. McDaniel Koch, F. Graf, S. Bajohr, R. Reimert and T. Kolb, *Renewable Energy*, 2016, **85**, 1371-1390.
154. S. P. Naik, T. Ryu, V. Bui, J. D. Miller, N. B. Drinnan and W. Zmierczak, *Chemical Engineering Journal*, 2011, **167**, 362-368.
155. J. Gao, C. Jia and B. Liu, *Catalysis Science & Technology*, 2017, **7**, 5602-5607.
156. Velocys Biorefineries, <https://www.velocys.com/our-biorefineries-2/>, (accessed 5/15/2019).
157. J. Wei, Q. Ge, R. Yao, Z. Wen, C. Fang, L. Guo, H. Xu and J. Sun, *Nat Commun*, 2017, **8**, 15174.
158. C. G. Visconti, L. Lietti, E. Tronconi, P. Forzatti, R. Zennaro and E. Finocchio, *Applied Catalysis A: General*, 2009, **355**, 61-68.
159. J. Wang, Z. You, Q. Zhang, W. Deng and Y. Wang, *Catalysis Today*, 2013, **215**, 186-193.
160. T. Herranz, S. Rojas, F. J. Pérez-Alonso, M. Ojeda, P. Terreros and J. L. G. Fierro, *Applied Catalysis A: General*, 2006, **311**, 66-75.
161. R. W. Dorner, D. R. Hardy, F. W. Williams and H. D. Willauer, *Applied Catalysis A: General*, 2010, **373**, 112-121.
162. T. Li, Y. Yang, C. Zhang, X. An, H. Wan, Z. Tao, H. Xiang, Y. Li, F. Yi and B. Xu, *Fuel*, 2007, **86**, 921-928.
163. W. Luc, M. Jouny, J. Rosen and F. Jiao, *Energy & Environmental Science*, 2018, **11**, 2928-2934.
164. F. Gallucci, L. Paturzo and A. Basile, *Chemical Engineering and Processing: Process Intensification*, 2004, **43**, 1029-1036.
165. U.S. Energy Information Administration: Electricity Data, <https://www.eia.gov/electricity/data.php>, (accessed 7/12/2019).
166. Flight: Facility Level Information on Greenhouse Gases Tool, <https://ghgdata.epa.gov/ghgp/main.do>, (accessed 5/28/2019).
167. BioFuels Atlas, <https://www.nrel.gov/gis/tools.html>, (accessed 7/12/2019).
168. National Research Council, *Climate Intervention: Carbon Dioxide Removal and Reliable Sequestration*, The National Academies Press, Washington, DC, 2015.
169. International Energy Agency, *CO2 Emissions from Fuel Combustion*, International Energy Agency, 2017.
170. American Physics Society, *Direct Air Capture of CO2 with Chemicals*, 2011.
171. S. Verma, B. Kim, H. R. Jhong, S. Ma and P. J. Kenis, *ChemSusChem*, 2016, **9**, 1972-1979.
172. K. Z. House, A. C. Baclig, M. Ranjan, E. A. van Nierop, J. Wilcox and H. J. Herzog, *Proc Natl Acad Sci U S A*, 2011, **108**, 20428-20433.
173. Y. Xu, L. Isom and M. A. Hanna, *Bioresour Technol*, 2010, **101**, 3311-3319.
174. 2019 Ethanol Industry Outlook, <https://ethanolrfa.org/wp-content/uploads/2019/02/RFA2019Outlook.pdf>.
175. L. Irlam, Global Costs of Carbon Capture and Storage: 2017 Update, <https://hub.globalccsinstitute.com/sites/default/files/publication/s/201688/global-ccs-cost-updatev4.pdf>, (accessed 5/28/2019).
176. J. Lau, G. Dey and S. Licht, *Energy Conversion and Management*, 2016, **122**, 400-410.
177. M. Johnson, J. Ren, M. Lefler, G. Licht, J. Vicini, X. Liu and S. Licht, *Materials Today Energy*, 2017, **5**, 230-236.
178. IHS Market Connect, 2019.
179. Bloomberg Finance L.P., 2019.
180. A. N. Chiramonti, R. M. White, J. Holm and E. Mansfield, *Microscopy and Microanalysis*, 2016, **22**, 450-451.
181. BP, *BP Statistical Review of World Energy*, BP, 2018.
182. Energy Information Administration, Natural Gas Henry Hub Natural Gas Spot Price, <https://www.eia.gov/dnav/ng/hist/rngwhhdA.htm>, (accessed 7/1/2019).
183. Methanol Institute, DME: An Emerging Global Fuel, <http://www.methanol.org/wp-content/uploads/2016/06/DME-An-Emerging-Global-Guel-FS.pdf>, (accessed 7/1/2019).

Broader Context

Transforming the Carbon Economy: Challenges and Opportunities in the Convergence of Low-Cost Electricity and Reductive CO₂ Utilization

R. Gary Grim, Zhe Huang, Michael Guarnieri, Jack R. Ferrell III, Ling Tao* and Joshua A. Schaidle*

*Corresponding Authors: joshua.schaidle@nrel.gov, ling.tao@nrel.gov

As we seek to globally transition from a linear carbon economy to a circular carbon economy, a key consideration is identifying the feedstocks and energy sources of tomorrow and developing the associated utilization technologies. As of 2018, we emitted more than 36 gigatonnes of CO₂ globally and reached more than 2,300 GW of installed renewable electricity generation capacity. Thus, an opportunity exists to utilize CO₂ and low-cost renewable electricity to drive this transition. CO₂ reduction technologies have been developed across direct and indirect approaches including electrochemical reduction, microbial electrosynthesis, non-thermal plasma, biological fermentation, and thermochemical hydrogenation. However, many of these technologies are at an early stage of development, and each one faces technical barriers that are impeding its commercial viability. In this contribution, we evaluate each of these five technologies to establish the current state of technology, describe the major technical barriers and R&D needs, and discuss near-term and long-term opportunities in the context of 22 accessible C₁-C₃ hydrocarbon and oxygenate products. Leveraging input from over 30 global subject matter experts, this perspective underscores the research opportunities and potential role of CO₂ reduction technologies in enabling our transition to a circular carbon economy.